Geophysical Journal International

Geophys. J. Int. (2010) **180,** 715–733 doi: 10.1111/j.1365-246X.2009.04428.x

The buried shape of an alpine valley from gravity surveys, seismic and ambient noise analysis

C. Barnaba,[1] L. Marello,[2,3] A. Vuan,[1] F. Palmieri,[1] M. Romanelli,[1] E. Priolo[1] and C. Braitenberg[4]

[1] *Istituto Nazionale di Oceanografia e Geofisica Sperimentale, INOGS–Borgo Grotta Gigante,* 42/c, *Trieste, Italy. E-mail: cbarnaba@inogs.it*
[2] *Geological Survey of Norway (NGU), Trondheim, Norway*
[3] *Department for Petroleum Engineering and Applied Geophysics (NTNU), Trondheim, Norway*
[4] *Dipartimento di Scienze della Terra, Universtità di Trieste, Trieste, Italy*

Accepted 2009 October 22. Received 2009 October 22; in original form 2008 April 9

SUMMARY

It has long been observed that damage due to earthquakes depends greatly on local geological conditions. Alpine valleys represent a typical populated environment where large amplifications can take place owing to the presence of surface soils with poor mechanical properties combined to complex topography of the rock basin. In the framework of the EU Interreg IIIB SISMOVALP Project 'Seismic hazard and alpine valley response analysis', a stretch of the Tagliamento River Valley (TRV), located in the north-western part of the Friuli Region (Italy) and close to the epicentre of the 1976 $M_w = 6.4$ earthquake, has been investigated with the aim to define the buried shape of the valley itself.

Two non-invasive, low cost, independent geophysical methods were used: (i) detailed gravity survey and (ii) H/V spectral ratio (HVSR) of microtremors.

Because of structural geological complexity and active tectonics of the Friuli region, an irregular valley shape was expected in this area. The independent analysis performed by gravity and passive noise, and complemented with refraction seismic velocity profiles, confirms this hypothesis and leads to two models that were consistent, but for some small scale details. The maximum depth estimated is about 400–450 m in the southern part of the valley, while a mean value of 150–180 m is estimated in the northern part. The sediment thickness obtained for this stretch of the TRV is quite large if compared to eastern Alps Plio-Quaternary rates; therefore the valley shape imaged by this study better corresponds to the top of carbonate rocks.

Finally, on the basis of the obtained morphology and some direct measurements, we conclude that the TRV features an overall 1-D seismic response (i.e. the resonance is related only to the sediment thickness rather than to the cross-section shape), but in its deepest part some limited 2-D effects could take place.

Key words: Gravity anomalies and earth structure; Earthquake ground motions; Body waves; Site effects; Wave propagation.

1 INTRODUCTION

The importance of local geological conditions and shallow site structure in sedimentary basins for seismic site response is well known and recognized throughout the scientific literature (e.g. Faccioli 1991; Aki 1993; Noganoh *et al.* 1993). Amplification mechanisms are well known and documented in many situations and their effects can be estimated quite accurately for the 1-D case (e.g. Sing *et al.* 1988; Borcherdt *et al.* 1989; Lermo & Chavez-Garcia 1993; Bonilla *et al.* 1997). However, mountain valleys often feature irregular morphology, sharp edges and high impedance contrasts which may give rise to pronounced 2-D to 3-D local effects that are usually strongly dependent on the seismic wavefield direction and very difficult to evaluate. In the last decades a large amount of numerical studies (e.g. Bard & Bouchon 1985; Sanchez-Sesma *et al.* 1993) and experimental observations (e.g. Field 1996; Steimen *et al.* 2003; Roten *et al.* 2006) demonstrated the importance of the detailed knowledge of the physical properties of shallow soils for interpreting the complex 3-D seismic response. To this aim, an accurate model for the subsurface structure should be obtained. Multicomponent reflection seismic and borehole surveys can provide an accurate subsurface image, however these methods are expensive and environmental impact is a concern especially in urban areas.

Alternative geophysical techniques, based on passive measurements and available at lower cost, are gravity surveying and the H/V

spectral ratio (HVSR) technique applied to ambient noise recording (Nakamura 1989).

The gravimetric method with dense acquisition surveys has been applied to alluvial basins or glacial valleys with the aim of imaging the shape of the underground bedrock and estimate the thickness of the sediments (Vallon 1999; Nishida *et al.* 2001; Møller *et al.* 2007). The success and accuracy of this approach is obviously linked to the presence of an appreciable density contrast between the bedrock and the sediments above as well as the availability of some external data (i.e. borehole data) to be used as a constrain for the inversion.

The HVSR method is nowadays extensively used within the geophysical community for estimating the fundamental resonance frequency of shallow soils. The technique, originally proposed by Kanai & Takanaka (1961) and based on a simple spectral analysis of microtremor measurements, was mainly improved by Japanese researchers in the following 30 yr as an exploration tool (e.g. Ohta *et al.* 1978; Kagami *et al.* 1982; Nakamura 1989; Akamatsu *et al.* 1992; Yamanaka *et al.* 1994). In the last 15 yr, several authors have investigated both the nature of the environmental noise and the phenomenology behind the HVSR in order to better understand the overall physics as well as to improve the processing techniques and its interpretation in term of underground structure (e.g. Tokimatsu *et al.* 1997; Bard 1998; Ibs-von Seht & Wohlenberg 1999; Delgado *et al.* 2000; Parolai *et al.* 2002; Fäh *et al.* 2003; Uebayashi 2003; Bard *et al.* 2004; Parolai *et al.* 2004; Di Giacomo *et al.* 2005; Bonnefoy-Claudet *et al.* 2006; Carniel *et al.* 2006; Fäh *et al.* 2007; Carniel *et al.* 2008; Herak 2008). Although the limits of the accuracy and applicability of this approach are still debated (Delgado *et al.* 2000; Bindi *et al.* 2001; Gueguen *et al.* 2007), it has became a common practice, under some simplifying conditions, to evaluate the thickness of soft sediments from the frequency of the HVSR main peak—if any—or even to invert the whole geological structure from the whole HVSR curve (Herak 2008), provided that some additional information on the geological structure is available.

Gravity data and ambient noise HVSR has been interpreted together with the aim of recovering the underground structure of alluvial basins only in few cases. Noguchi & Nishida (2002) determined the subsurface structure and shape of the Tottori Plain by considering together the information coming from residual gravity anomaly, HVSR curves, and *S*-wave velocity structure derived from array records of noise. Few studies of joint inversion of gravity data and surface wave velocities (Hayashi *et al.* 2005; Maceira & Ammon 2009) are performed to define geological features. Gueguen *et al.* (2007) pointed out for a very investigated area such as the Grenoble basin that the effects of deeply engraved basins (i.e. with small apex ratio) can disturb the estimation of the fundamental frequency of vibration made by the HVSR method and therefore mislead the interpretation of the bedrock depth especially at the basin edges, where subsurface layers are characterized by larger heterogeneities and where the basin topography is accentuated.

This study has been carried out within the Interreg IIIB SISMOVALP Project of the European Union (http://www.alpinespace.org/sismovalp.html). The general aim of this project was that of improving the overall knowledge of the seismic hazard for the alpine valleys in order to reduce the vulnerability to earthquakes in the alpine space. One of the workpackages was devoted to gather and organize old and newly acquired geological and geotechnical data into a transnational geotechnical database for a number of 'pilot' valleys (Lacave *et al.* 2006). Then, starting from the evidence that all alpine valleys comes from the same orogenic process and share the same geological evolution (Lemeille 2004), it was possible to identify some common features and draw some generic characterization, including some 'generic' models, to be used for other alpine valleys where detailed information is missing (Lacave & Lamille 2007).

Within this framework, this paper presents the case-history on a stretch of the Tagliamento River Valley (TRV), between Tolmezzo and Cavazzo Carnico municipalities, in the northeastern part of the Friuli-Venezia Giulia Region (NE Italy). The area is close to the epicentre of the 1976 ($M_w = 6.4$) Friuli earthquake and it was struck in the past by several earthquakes of $M > 5.5$.

A first 3-D model of the buried shape of the valley and the application of low-cost and low-impact methods suitable to define it, represent the main goals of this paper. In this study, gravity and ambient noise HVSR methods have been considered separately in order to get mutual benefit of the independent pieces of information provided by them. Hereinafter, all the geological and geotechnical information available for this area and the results obtained from shear wave profiling, gravity measurements and ambient noise recordings are presented. The comparison between the results obtained separately by interpreting both gravity anomalies and fundamental frequencies estimated from HVSR provide a first image of the seismic rock basement in this sector of the TRV.

2 GEOLOGICAL/GEOTECHNICAL SETTING AND INITIALLY AVAILABLE DATA

The study area is located in northeastern part of Italy, in the TRV, between Tolmezzo town (TZT) and Cavazzo Carnico plain (CCP) (Fig. 1). The flood plains of Tagliamento river and its tributary, the But river, are surrounded by Permo-Triassic carbonate rocks of Mt Strabut, Mt Amariana and Curions Hill. A small outcrop of Carnian shallow-water deposits (thinly laminated dolomites, marly sandstones and gypsum) is also present north of Curions Hill, and buried under the Rivoli Bianchi fan (Ponton, personal communication, 2008). The Tagliamento conglomerate, a polygenic and heterometric carbonate alluvial deposit of middle-upper Pleistocene age, outcrops on the right side of the valley—the river flows from NW to SE in the figure, while alluvial fans of cobbles and gravels characterize the left-hand side of the area (Carulli 2007).

Tectonics plays an important role in the area: normal faults and thrusts are evidenced in geological surface mapping. Most of them are hypothesized to be buried under the Quaternary coverage, and their geometrical characteristics and age are not easy to interpret. According to Carulli (2000) the structural pattern is very complex and three main directions of faulting have been identified (i.e. NNE–SSW, E–W and SE–NW, respectively).

This area is close to the epicentre of the 1976 Friuli earthquake ($M_w = 6.4$) and was struck by several earthquakes in the past (Ambraseys 1976; Slejko *et al.* 1987). In addition, it is densely inhabited and a large chemical plant and many small-scale productive assets are located in the southern part of Tolmezzo on the Quaternary deposits.

Although several borehole measurements and hydrogeological and geotechnical investigations were available, the knowledge of the soils and underground structure of the valley was very poor. A large number of these investigations are dated back to the 1976 Friuli earthquake rebuilding. Most of them penetrated only the shallow soils, up to a maximum depth of 10 m, while for several boreholes that were drilled in the 1960s the stratigraphic description is not available. No boreholes reach the hard rock within the valley and

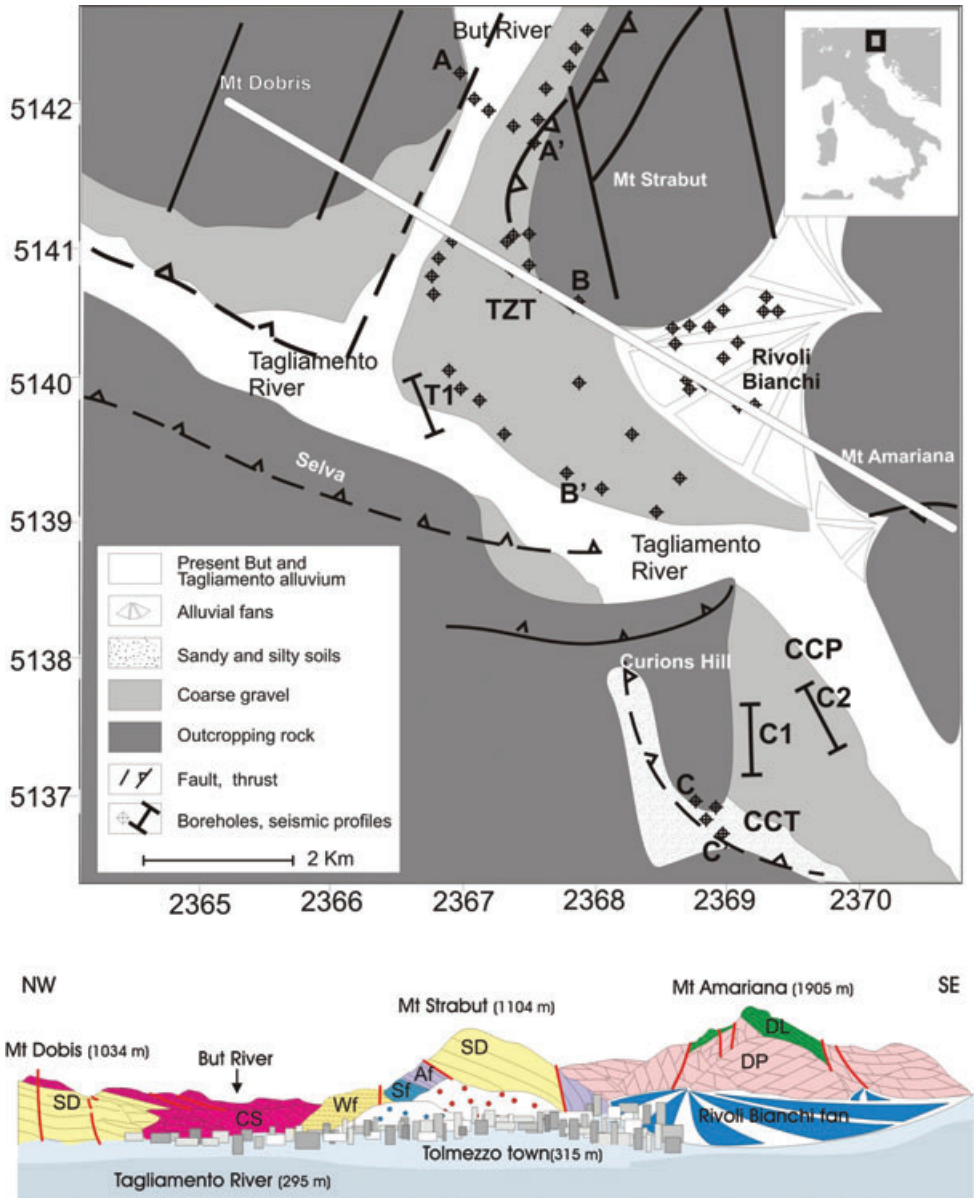

Figure 1. Top panel: sketch of the Tagliamento River Valley (North Eastern Alps, Italy) study area. Lithology, main tectonic elements (from Carulli 2007, simplified), boreholes and *S*-wave velocity surveys are mapped (TZT, Tolmezzo town; CCP, Cavazzo Carnico Plain; CCT, Cavazzo Carnico Town). AA′, BB′ and CC′ show the position of Fig. 2 stratigraphic boreholes. The coordinates are given in kilometres of the Italian coordinate system (Gauss–Boaga system). Bottom panel: perspective geological section of the outcropping rocks (from Carulli & Ponton 2002, redrawn and simplified). The location of the section is shown by the thick white line in the map. The abbreviations indicate the main geological formations: SD, Wf, Sf, Af: shallow water carbonate platform deposits; CS: dark grey limestones; DL, DP: limestones and massive dolostones.

no detailed seismic reflection line pass across it. Moreover the few available pieces of information on the *S*-wave velocities and density of shallow soils was limited up to 10–20 m and not always reliable.

Only in the northern part of the Tolmezzo, the bedrock is better identified. Thanks to five drills that penetrate the soil along the But River Valley and are aligned along a transversal direction (AA′ in Figs 1 and 2 top panel) it is possible to sketch a limestone bedrock dipping gently to W along the eastern (i.e. left-hand) side of the valley (A′ in Figs 1 and 2), with maximum observed depth of about 60 m. The borehole in the middle and middle-left part of the river bed, 148 and 104 m deep, respectively, do not reach the hard rock; however on the base of the surface topography it is possible to infer a possible maximum bedrock depth of about 180 m. Along this section, the sediment fill is represented by cobbles and gravels with small percentage of sands.

Softer sediments are found in the Cavazzo Carnico area (CCT in Figs 1 and 2 bottom panel), at the right edge of the valley and southern part of the investigated area. Representative lithologies and stratigraphy can be derived only from shallow drills located in the western part of the village where fine sands and clays are found. A deeper borehole at the edge of the plain evidences the presence of carbonate bedrock at 20 m of depth (Bressan 1981). At present, no other information is available for the bedrock in this area. A GPR survey has recently been carried out by the University of Basel to detect the shallow sedimentary pattern. The preliminary results show that sediments in this area consist mainly of fine, horizontally

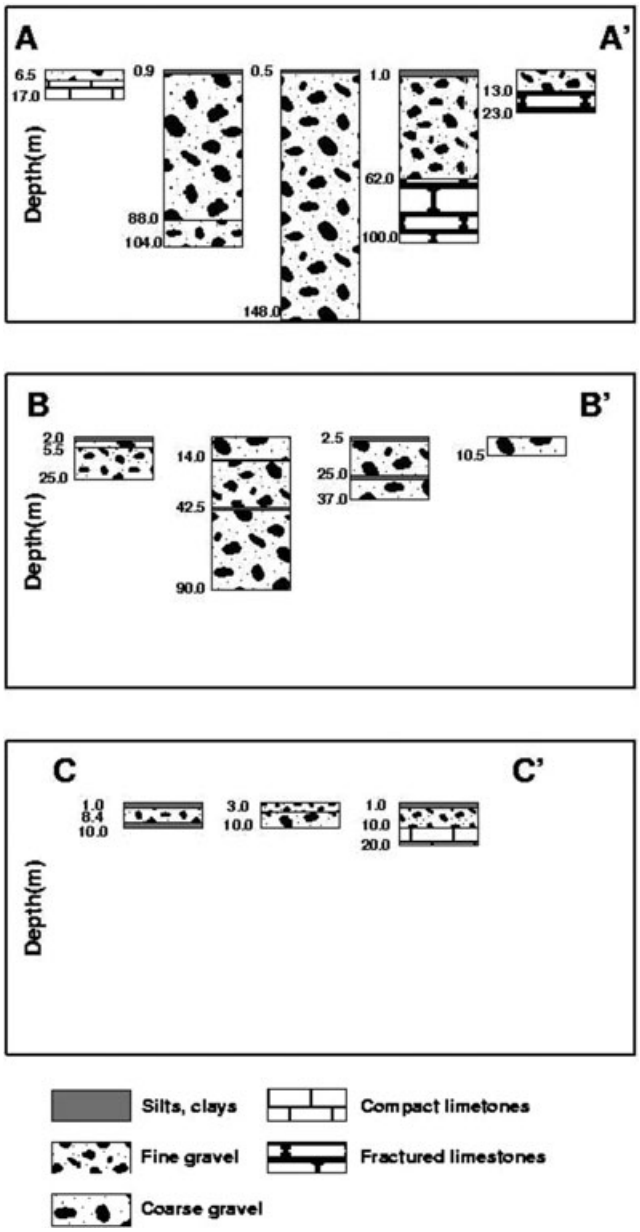

Figure 2. Stratigraphy of the three borehole groups: AA′ (top panel; location across the But River, in Fig. 1), BB′ (middle panel; location within the Tolmezzo town) and CC′ (bottom panel; location within Cavazzo Carnico town).

layered strata, often with a high content of clay rather than gravels (Pfister, personal communication, 2007).

3 *S*-WAVE VELOCITY PROFILING

In order to better characterize the seismic properties of the shallow soils (i.e. unconsolidated sediments) of the TRV, *S*-wave array measurements have been carried out by analysing and inverting the dispersion curves of Rayleigh and Love wave's fundamental and higher modes. Seismic signals are induced by an active seismic source. Three sites (C1, C2 and T1) have been investigated: their location is shown in Fig. 1, while the seismic acquisition parameters and geometry used are described in Table 1 (note that the acquisition parameters adopted for T1 are different from those of C1 and C2). The acquisition has been performed using an array of six seismic stations equipped with three components 1 Hz sensors. Multiple weight drops were used to record redundant seismic data. The layout of the seismic profiles was oriented along the longitudinal axis of the valley, in order to meet the physical conditions of 1-D medium and remove apparent surface wave arrivals. The vertical and transverse components of the recorded waveforms at sites C1, C2 and T1 are shown in Fig. 3. All the seismic sections show a well developed ground roll fan, with coherent surface wave dispersion typical of the propagation through a 1-D layered medium.

A 2-D transform has been applied to the recorded wave field to enhance the detection and separation of the surface wave phase velocities. The algorithm was developed by Herrmann (2005) and follows the formalism described by McMechan & Yedlin (1981). The phase velocity dispersion curves are obtained from an array of seismic traces by using a $p - \tau$ stack followed by a transformation into the $p - \omega$ domain. Fig. 4(a) shows the Rayleigh and Love wave dispersion diagrams used for the determination of the fundamental and higher modes for the three investigated sites. Since the seismic line spread for T1 is larger than for C1 and C2, the T1 dispersion curves are measured by using data recorded at 110–280 m of offset from the source.

The interpreted modes, in terms of frequency—phase velocity values and associated standard error, are shown in Fig. 4(b). The phase velocity error Δc comes directly from the value of the coherence function (i.e. the stack values). It is proportional to the square of the phase velocity, according to the relation $\Delta c = \sigma c^2$, where σ is the standard error of the ray parameter normal distribution estimated from the coherence function in the frequency—phase velocity domain. More details about the error estimation can be found in Herrmann & Ammon (2002). The phase velocity error ranges from about 5 to 300 m s^{-1} for the high and low frequency bands, respectively. In per cent units, the error ranges from a minimum of about 2 per cent to a maximum about 35 per cent; the average error is of about 10 per cent. Since accurate phase velocity measurements have been obtained in the frequency band ranging from 3–4 to 30 Hz, reliable *Vs* models can be determined down to a depth of about 120–130 m at all sites. This depth is useful for either constraining the shallow sediments average *S*-wave velocity and for defining the bedrock velocity at the valley edge (C1).

The Rayleigh and Love phase velocity curves are used jointly to determine the *Vs* structure of the sediments by applying a linearized inversion scheme (SURF96, Herrmann & Ammon 2002). The initial starting models are derived from a seismic refraction analysis of the same data (see Fig. 3) using two different options (see Xia *et al.* 1999, and Luke & Calderon-Macias 2007), that is,

(1) Manual selection of all the layer parameters accordingly with the seismic refraction profiles.

(2) The number of layers N and the thickness increasing ratio are selected by taking into account the rules of thumb described in Xia *et al.* (1999).

To limit the number of inversions, an inversion procedure is followed close to that described by Cercato (2009), where dispersion curve sensitivity with respect to perturbations applied to layer parameters is checked together with initial model misfit. This kind of selection of the input model parametrization, together with a smoothing constrain that prevents large variations between layer velocities, guarantees the robustness and stability of the inversion algorithm. In order to evaluate the stability of the results and the error induced, several inversion runs of 10–20 iterations each have been performed using different starting models as well as different

Table 1. Main acquisition parameters used for seismic site characterization of sites C1, C2, T1.

Site	Source weight(kg)–height(m)	Offset interval (m)	Intergeophone distance (m)	Geophone natural frequency (Hz)
C1	120–3	10–130	1	1
C2	120–3	10–130	1	1
T1	600–6	80–480	10	1

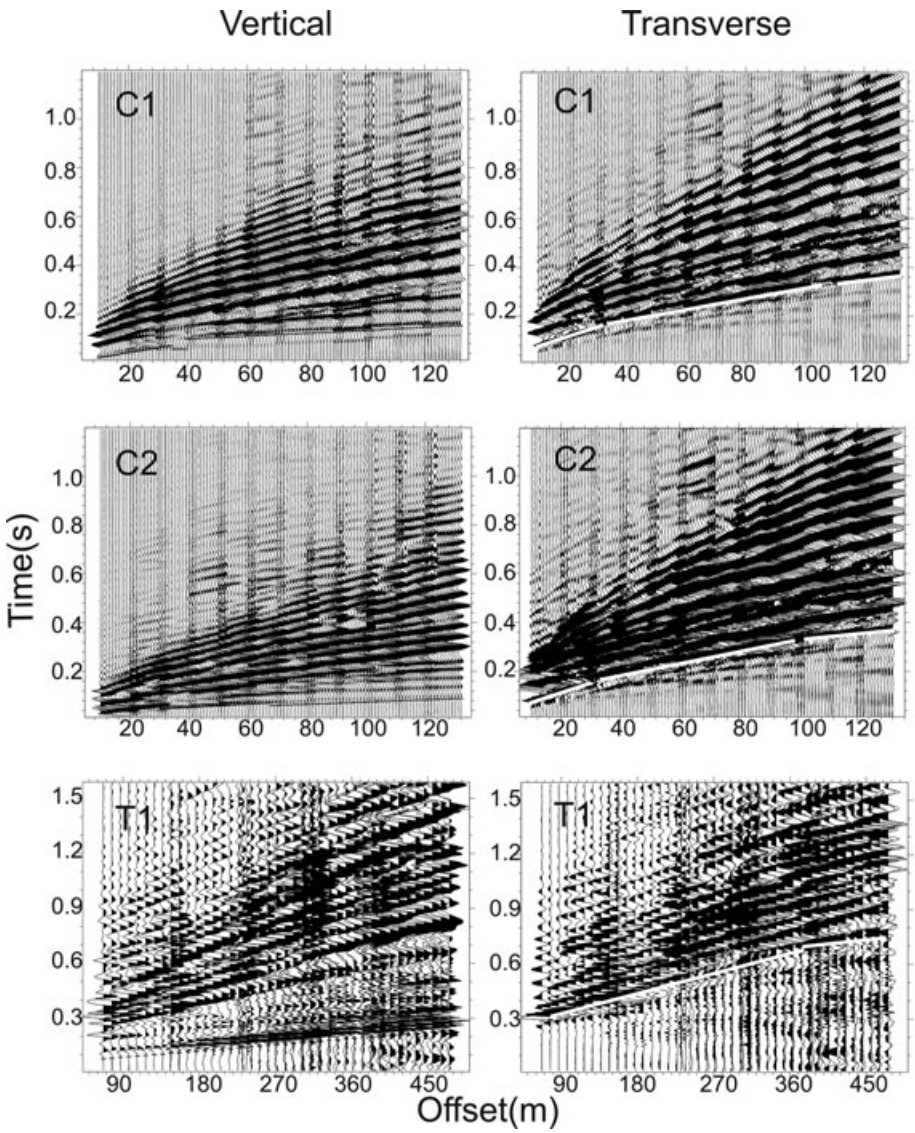

Figure 3. Seismic recordings of the vertical (left-hand panels) and transverse (right-hand panels) components at C1, C2 and T1 sites (see Fig. 1 for location). The seismic arrays are deployed parallel to the longitudinal axis of the valley (i.e. parallel to valley direction): in this way the surface wave trains, identified by a white line, are well correlated for all the offsets.

smoothing and damping values. The constrained linear inversion provides a number of possible models, which display sharp velocity contrasts or velocity gradients and feature theoretical dispersion curves consistent with the observations. For all the resulting models, the main features (i.e. peaks and throats) of HVSR from microtremors at nearby sites are then matched with the Rayleigh wave ellipticity curves computed from the inverted *S*-wave velocity models (Herrmann 2005). *S*-wave velocity models at the three sites are selected on the basis of the consistency between the main peaks/throats of computed transfer functions (ellipticity curves for the Rayleigh waves) and the HVSR curves.

Fig. 5 compares the preferred *S*-wave models with the models derived from refracted *S*-wave arrival peaks. The standard deviation estimated for the models defined from the surface wave velocity analysis is of about 10–25 per cent the average value. Uncertainties related to *Vs* profiling are determined by considering several different parametrizations of the initial model for the inversion procedure, that is, number of layers, level of smoothness of the allowed perturbations and *Vp*/*Vs* dependence. The three investigated sites feature somewhat different *Vs* profiles. Site C2, in the middle of the valley, has a slowly increasing velocity with depth from about 800 to 1200 m s^{-1}, but for the shallowest 15 m. No strong velocity

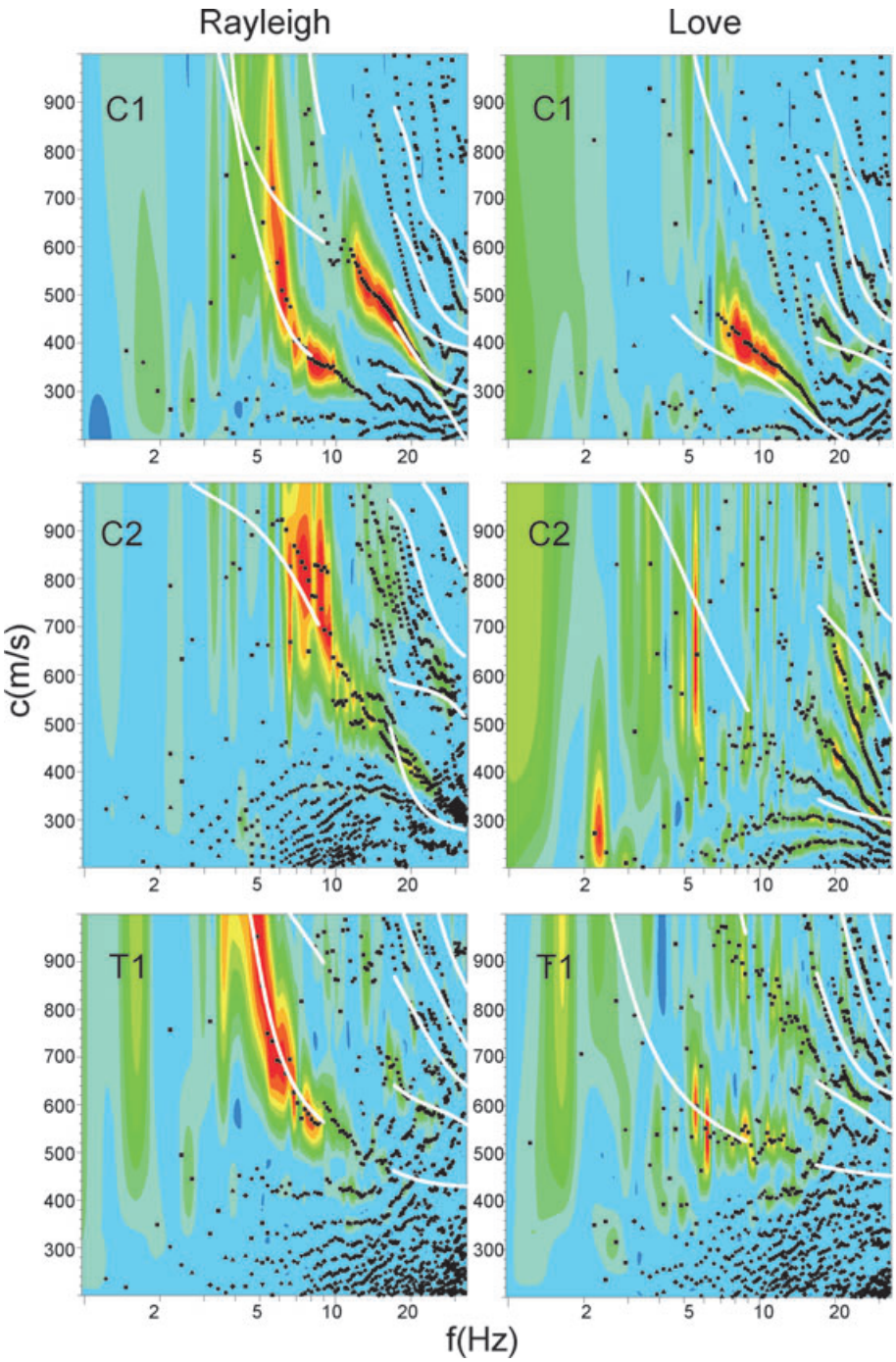

Figure 4. (a; this page) Phase-velocity stack values of the seismic data shown in Fig. 3. The colours indicate the stack value (the largest values in red). The black symbols represent the peaks chosen from the stack after a 2-D search over the phase velocity–frequency grid. The solid white curves represent the theoretical Rayleigh (left-hand panels) and Love (right-hand panels). (b; next page) Rayleigh (left-hand panel) and Love (right-hand panel) fundamental and first higher mode wave dispersion diagrams for the three investigated sites in terms of frequency–phase velocity effective picked from the f–c spectrum of Fig. 4(a). Error bars are estimated using the procedure described in Herrmann & Ammon (2002) and based on the value of the coherence function.

contrasts are detected within the maximum depth of investigation. On the other hand, both sites C1 and T1, which are located at the edge of the valley although in two different areas, reveal lower velocity values of about 600 m s^{-1} for a 60-m-thick portion of shallow sediments. These velocity values are consistent with those found in the literature for gravelly soils and coarse sediments at shallow depths (Pedersen *et al.* 1995; Frischknecht & Wagner 2004; Havenith *et al.* 2007). It can be also noticed that the three profiles feature quite similar velocity values in the shallowest portion of unconsolidated sediments, that is, above the first velocity contrast, independently of the position of each site within the valley. Fig. 6 shows how the resulting models match the HVSR curves of ambient noise, acquired at the three sites (see also Section 5). Note that both the main peaks/throats of computed transfer functions and singularities of the ellipticity curves for the Rayleigh waves do correspond to those of the HVSR for frequencies larger than 1–2 Hz.

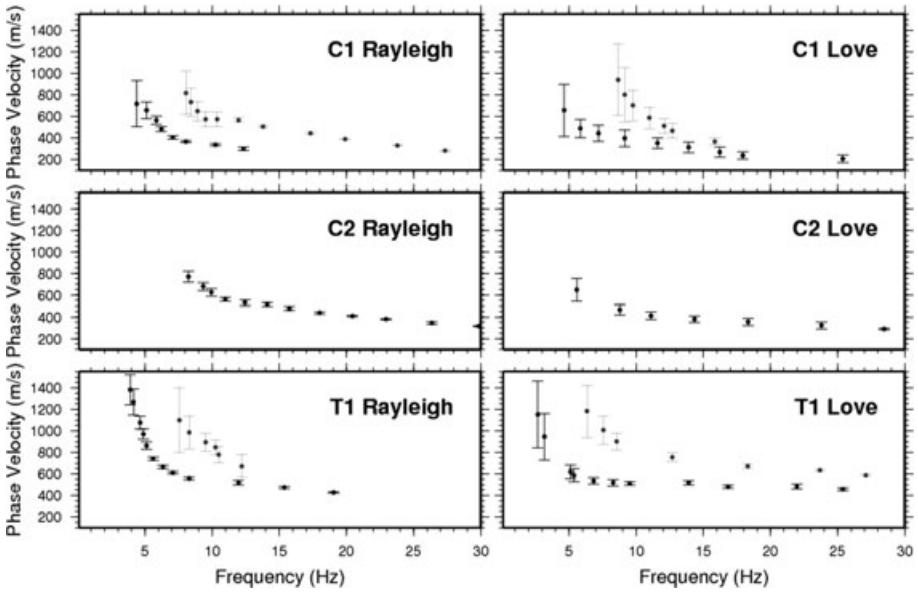

Figure 4. (*Continued.*)

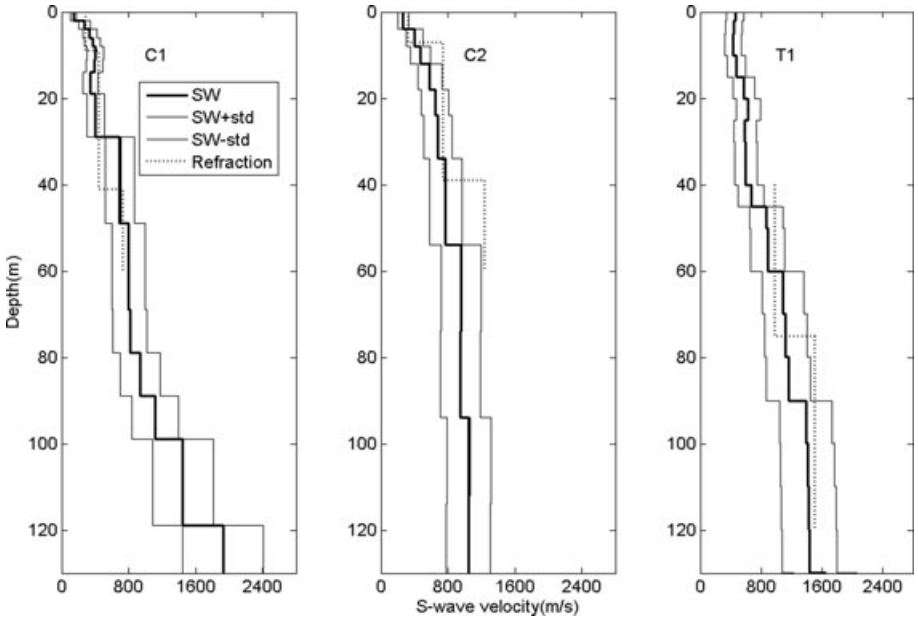

Figure 5. *S*-wave velocity versus depth obtained at sites C1, C2 and T1 from the surface wave velocity inversion (black lines; the thick and thin curves represent the average and average ± the first standard deviation, respectively) and seismic refraction interpretation of the first *S*-wave arrival peaks (dotted line).

4 VALLEY MODEL FROM GRAVITY DATA

4.1 Gravity survey

A detailed gravity survey has been carried out in the study area. A total of 266 gravity stations (see Fig. 7 for the layout of measurements), spaced about 200 m, have been measured with a Lacoste & Romberg (L&R) gravity meter model D, equipped with a feedback developed by Zero Length Spring (ZLS). A first order gravity net has been established and it has been tied to the absolute gravity station of Trieste.

The data acquisition of the gravity survey followed the looping technique in order to monitor the instrumental drift, that span from -0.002 to $+0.002$ mGal h^{-1} (1 mGal $= 10^{-3}$ Gal, 1 Gal $=$ 0.01 m s^{-2}) and to assess the loops' error closures, that span from -0.003 to $+0.003$ mGal. Besides, to check the instrumental repeatability, roughly 10 per cent of the stations have been remeasured: the results show that 80 per cent of the resulting gravity differences lie in the interval ± 0.004 mGal.

The gravity data resulted from the network adjustment has been used to calculate the Bouguer gravity anomaly, following standard techniques (La Fehr 1991a):

(1) Geodetic Reference System 1980 for the normal gravity.
(2) Free air correction, up to 2nd order in height.
(3) Bouguer correction considering also the Bullard B term that takes into account the Earth's curvature (La Fehr 1991b).
(4) Terrain correction, considering vertical right prisms (Banerjee & Das Gupta 1977), up to 25 km with curvature

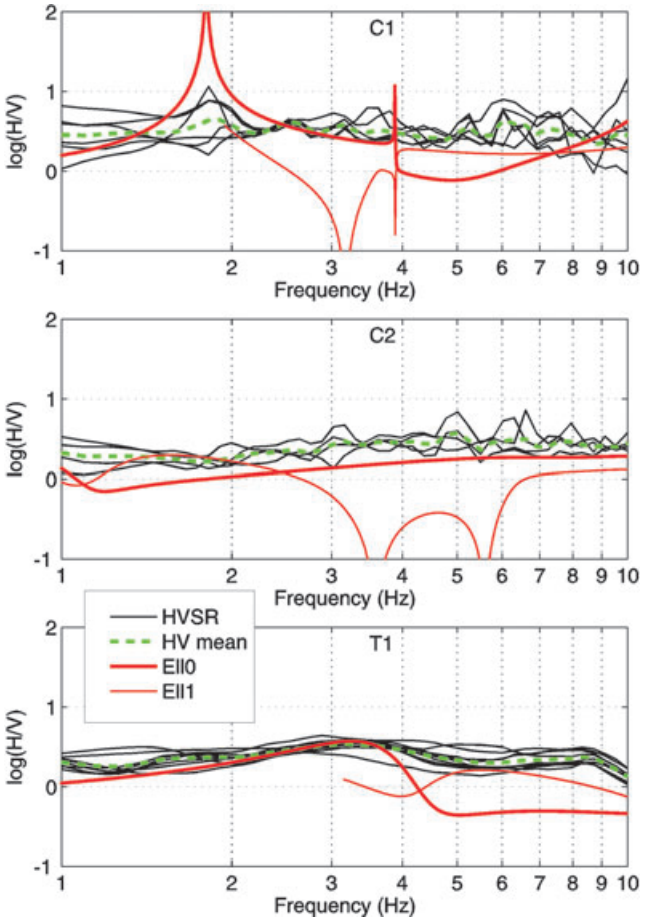

Figure 6. Comparison of the HVSR of ambient noise (dashed lines), theoretical transfer function (blue bold line), and ellipticity of some Rayleigh modes (red solid lines) computed for the reference models of C1, C2 and T1 sites (see Figs 1 and 8 for the site location and reference models, respectively). The green bold dashed line represents the mean value of the observed HVSR curves (thin dashed lines). The ellipticity is represented for the fundamental (Ell0, red thick solid line) and first higher (Ell1, red thin line) Rayleigh modes.

correction beyond 18 km, using several DTM cell size according to the distance from the gravity station.

All the above mentioned calculations have been carried out using a density of 2500 kg m^{-3}. Therefore, considering the errors that arose from the data acquisition and processing, an error of $\pm$0.015 mGal has been estimated on the Bouguer anomaly.

The Bouguer anomaly map (Fig. 7a) presents a regional trend with a northward negative regional field. It is probably dominated by the effect of northward isostatic crustal thickening due to the increasing alpine topography (e.g. Braitenberg *et al.* 2002; Ebbing *et al.* 2005; Zanolla *et al.* 2005). As the regional signal masks the local signal generated by the shallow sediments, the regional field has been removed.

In order to isolate the regional signal different filtering and mathematical functions have been tested. The second-degree polynomial expression of the Bouguer anomaly field (Fig. 7b) results to be the most appropriate regional field, since it reproduces well the NS trend and is not correlated with the morphology of the valley. The residual anomaly map obtained (Fig. 7c) features the shallower density variations (present and past river beds, lateral fans and carbonate rock highs). The gravitational effect due to the TRV and But Valley is clearly recognizable as the residual negative anomalies. The lowest negative residual values could be related to the thick alluvial sediments dominated by low density and located at the bottom of Rivoli Bianchi fan and the CCP. The higher positive residual anomalies are located near Mt Dobis (NW corner of the map), Curions Hill (southwestern part of the map), and the western edge of Mt Amariana (eastern part of the map), where compact carbonate rocks outcrop.

4.2 Gravity modelling

The subsurface structure of the valley has been investigated by interpreting the second order polynomial residual anomaly using 3-D forward modelling technique (IGMAS, Götze & Schmidt 2005). The modelling procedure is based on 'trial and error' method. The algorithm used for gravity field calculation discretizes the volume into tetrahedral (Gotze 1978). The 3-D geological bodies in the model are bounded by triangulated surfaces (layer boundaries), which limit domains with constant density. These triangulated surfaces are defined by polygons along several vertical 2-D sections parallel each other (Fig. 8). The construction of the final 3-D model structure is then performed automatically by IGMAS from the 2-D sections. Interactive modification of the model parameters (i.e. geometry and density) is performed through a direct, simultaneous visualization of both the calculated and measured gravity. Once the gravity is computed for the 3-D model, the computed and observed residual anomalies are compared each other, and the modelling process starts again with another step or stops in the case of good convergence. At a preliminary stage, some tests have to be performed in order to define the most suitable number of sections and bodies, the density values, and the initial geometry.

The model here presented as the 'final model' (Fig. 7d) is the most accurate one obtained after the whole iterative process. Its geometry is defined along 16 NS sections spaced by about 200 m in the denser part (Fig. 8a). The 3-D structure consists of five 3-D bodies with constant density. Table 2 summarized the characteristics of each body, while one of the vertical sections used for defining the model is shown in Fig. 8(b). The starting density values have been assigned mainly on the basis of literature data specific for the alpine environment (Lacave & Lamille 2007). The alluvial/glacial sediments are divided into two different bodies (i.e. layers) representing unconsolidated and consolidated sediments, respectively. A specific constrain for the shallow sediments of this study comes from bibliography *Vp* velocity value measured in shallow refraction seismic survey located in the northern area of Tolmezzo municipality which falls in the range 1100–1370 m s^{-1} (Petris 1996). The density range of 1780–1850 kg m^{-3} obtained after conversion (Gardner *et al.* 1974) agrees with those of literature and has been used for the top-sediments. For the consolidated sediments, the density has been selected on the base of the indications provided by SISMOVALP project (SISMOVALP Project – WP6 Generic alpine ground motion 2007) and agree with those adopted in the other few similar studies performed for alpine valleys (e.g. Frischknecht *et al.* 2005). The goodness of this approach is supported by the comparison between the density vertical profiles of the final model and those obtain converting the *Vs* profiles acquired in this study. Fig. 8(c) shows the results: the solid line represents the density values derived from the new acquired *Vs* using empirical conversion laws applied in two sequential steps, that is, from *Vs* to *Vp* (Brocher 2005) and then from *Vp* to density (Gardner *et al.* 1974). The dotted line shows the final density values obtained by 3-D forward gravity modelling.

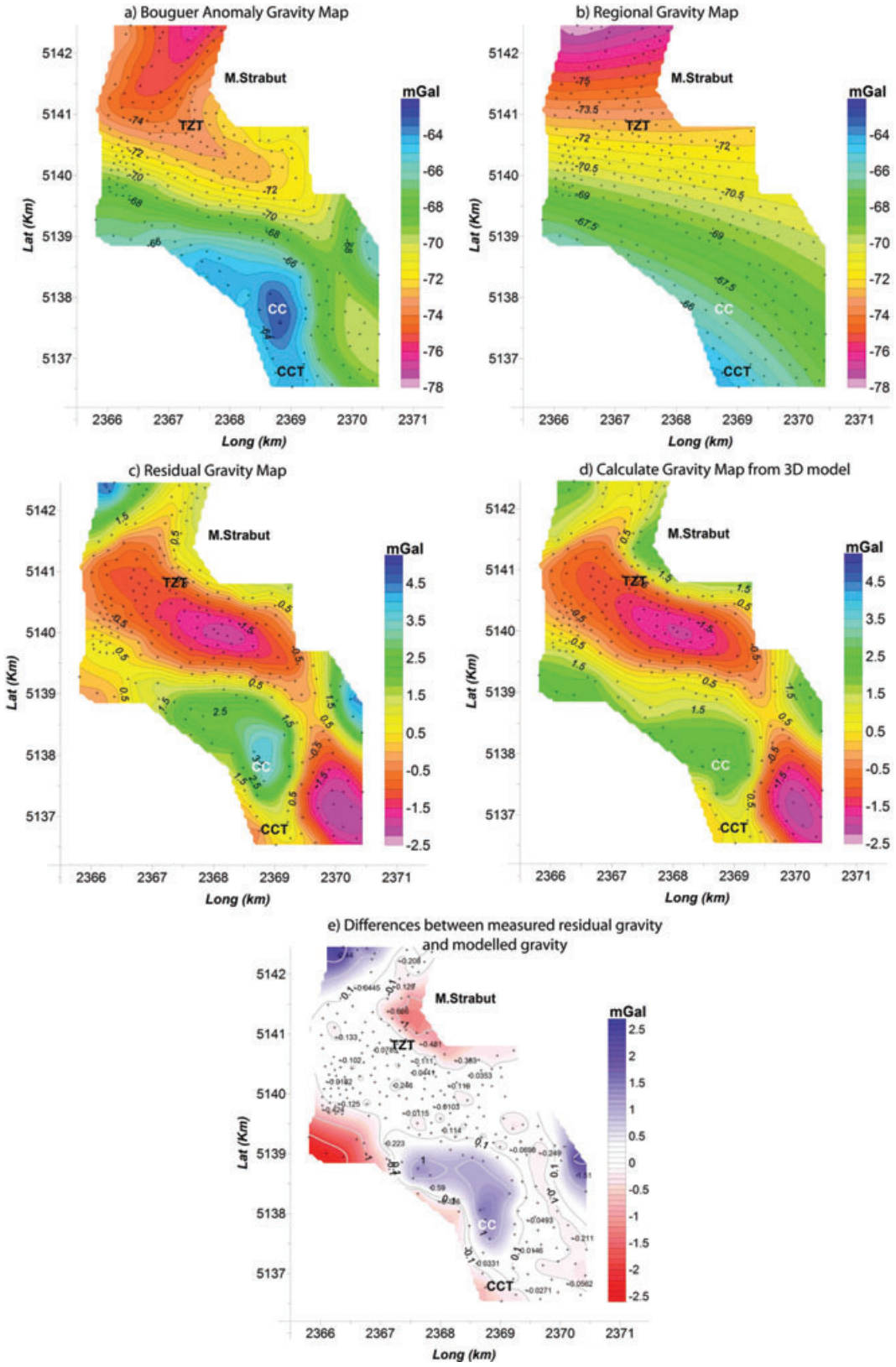

Figure 7. Bouguer anomaly map (a), regional gravity field (second degree polynomial definition of the Bouguer anomaly) (b), residual gravity field (c), residual gravity calculated from 3-D model (d), and difference between measured and modelled residual gravity fields (d). The difference values are explicitly written at some measurement points in panel (d). Black dots indicate the measurement points. Coordinates are given as in Fig. 1.

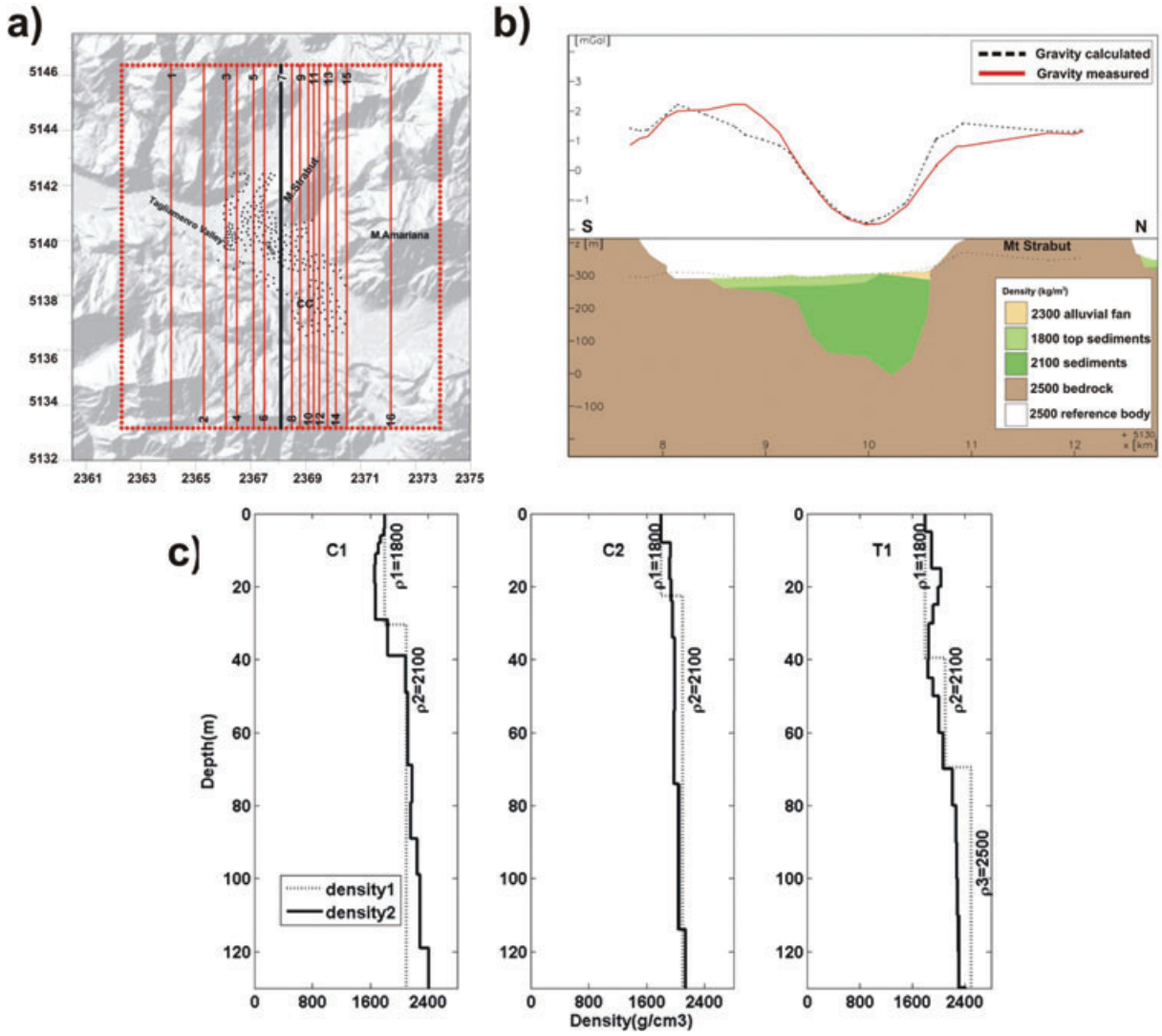

Figure 8. (a) Plan of the 2-D transects used to define the 3-D gravity model with IGMAS. The final model is defined by 16 sections; (b) for each section IGMAS calculates the gravity field and displays the computed and observed gravity anomaly. The example shown here highlights the misfit obtained at the valley edge owing to a inadequate value of bedrock density: at south, the adopted density value of 2500 kg m^{-3} is lower than the real one, while the contrary happens at north. (c) comparison between the density final model (dotted line) and the density profiles derived from the new acquired *Vs* using empirical conversion laws (see text for more details).

Table 2. Parametrization of the gravity model.

	Geological description	Depth (m)	Density (kg m^{-3})
Body 1	Top alluvial sediments (unconsolidated clays and sands)	0–30m	1800
Body 2	Alluvial sediments (consolidated clays and sands)	>30m	2100
Body 3	Alluvial fans	–	2300
Body 4	Bedrock (carbonatic rocks)	–	2500
Body 5	Reference density	–	2500

In order to define the model gravity anomaly, a reference model must be chosen. A reference density of 2500 kg m^{-3} has been used, which corresponds to the value adopted for the Bouguer anomaly calculation and the value assumed for the valley bedrock. Thus, the resulting anomaly represents only the effect of the shallower modelled bodies (loose sediments and alluvial fans). In the manual iterative process, the parameters that have been changed are boundaries (among sediments-basement and sediments-fans) and densities (of the loose sediments and fans).

The main density contrast is defined between the alluvial deposit and the underlying rock (carbonate rock). The interface between consolidated and unconsolidated sediments is defined at 30 m of depth. In the iterative process, the depth of this interface has been held fixed while the density of the top sediments has been left to vary within the range indicated above. No lateral density variation (i.e. from the centre to the edge of the valley) has been introduced, since the available data (e.g. the already mentioned GPR survey and the borehole description) do not allow to improve the adopted

plane layer model in this sense, but arbitrarily (Pfister, personal communication, 2007). The value of 1800 kg m^{-3} (Table 2) is the final result of the iterative modelling process obtained for the top sediments. The geometry of the other buried boundaries (bedrock-valley sediments, bedrock-fans and fans-loose sediments) as well as the density of the alluvial fan is the result of the iterative procedure of modelling, since no other constraint is available at present.

For the final model, the shape of the calculated gravity anomaly field is well correlated with the measured field (correlation coefficient equal to 0.90). The difference between the measured and calculated gravity anomaly fields (Fig. 7e) always is lower than ±0.2 mGal, that is, less than 3 per cent of the measured residual gravity anomaly, within the valley. It becomes significant (with values of about ±2 mGal) only at the border of the study area where the bedrock outcrops, that is, at the foot of Mt Dobis, at and near the Curions Hill, and at the foot of Mt Strabut. These discrepancies are an effect of the difference between the real density distribution in the bedrock versus the one defined in the model: positive/negative values correspond to higher/lower density than the assumed one. Thus the formations of the Curions Hill, Mt Amariana and Mt Dobis feature density higher than 2500 kg m^{-3}, while the opposite holds for Mt Strabut and the hills SW of Tolmezzo. This result agrees with the observed lithologies, as the dolomite of the Curions Hill and Mt Amariana is expected to be denser than the other surrounding formations (Faccenda *et al.* 2007).

The morphology of the TRV resulting from the gravity interpretation is displayed in Fig. 9. It shows two deeper trenches with maximum depth of 400–450 m, one located at SE of Tolmezzo, between Mt Strabut and Curions Hill, and the other at East of Cavazzo Carnico, at the edge of the study area.

The study here presented aims at providing a first image of the buried morphology of the TRV, hence the accurate modelling of the rock structure, in order to get rid of the discrepancies obtained in the residual gravity anomaly already discussed, and possible consequences in terms of tectonics are out of the scope of this paper. However, some tests have been performed in order to evaluate the error on the reconstructed shape of the valley. It has been found that the reconstructed valley shape is rather stable and its depth depends mainly on the density contrast between bedrock and alluvial sediments, that is, the lower (higher) the density contrast between the bedrock and alluvial sediments the deeper (shallower) and narrower (wider) becomes the valley. In particular, a variation of ±100 kg m^{-3} in the density contrast between the bedrock and the alluvial sediments—considering that the reference density contrast is 400 kg m^{-3} (Table 2), this value corresponds to a variation of about 25 per cent and represents an upper limit of the uncertainty—results in a maximum variation of about ±70 m in the deeper parts of the valley (CCP), that is, less than 20 per cent of the maximum depth.

5 VALLEY MODEL FROM MICROTREMORS

Ambient seismic noise has been recorded at 260 sites throughout the valley (Fig. 10), with major detail in the areas of TZT and CCT. The recording equipment consisted of a Reftek C130 station with a three-component 1 Hz sensor (Lennartz 3-DLite/1 s). The recording duration ranges from 20 to 60 min, in order to ensure good quality signal windows. About 10 per cent of the measurements were repeated 2 yr later for verifying the stability of the results. When possible, the measurements were performed at or close to the sites where borehole data were available.

All the recorded data have been analysed using the single station H/V method. A manual selection of the time windows has been performed in order to retain the most stationary parts of noise and avoid anomalous spikes or transients often associated with specific sources (e.g. walking, traffic). The spectral analysis was performed on multiple cosine tapered 180 s long windows of the signal. The overall processing procedure is consistent with the recommendations of the SESAME Project (2004). More details can be found in Priolo *et al.* (2001).

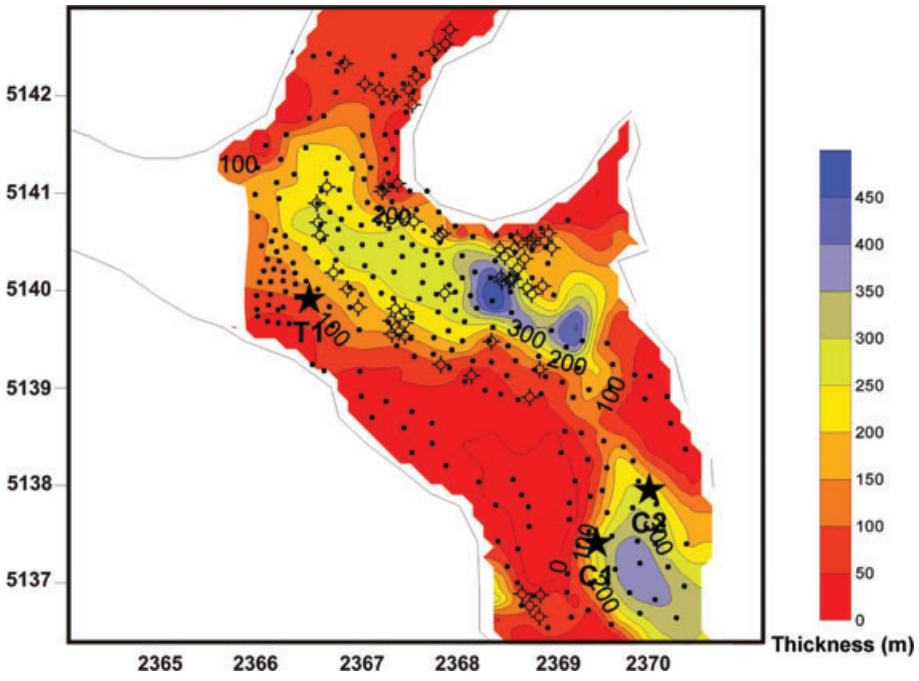

Figure 9. 3-D IGMAS model of the buried morphology of the Tagliamento River Valley. The thickness of the sedimentary coverage above the geophysical bedrock is obtained by interpolating the results of gravity modelling. The location of the boreholes and seismic profiles is explicitly shown.

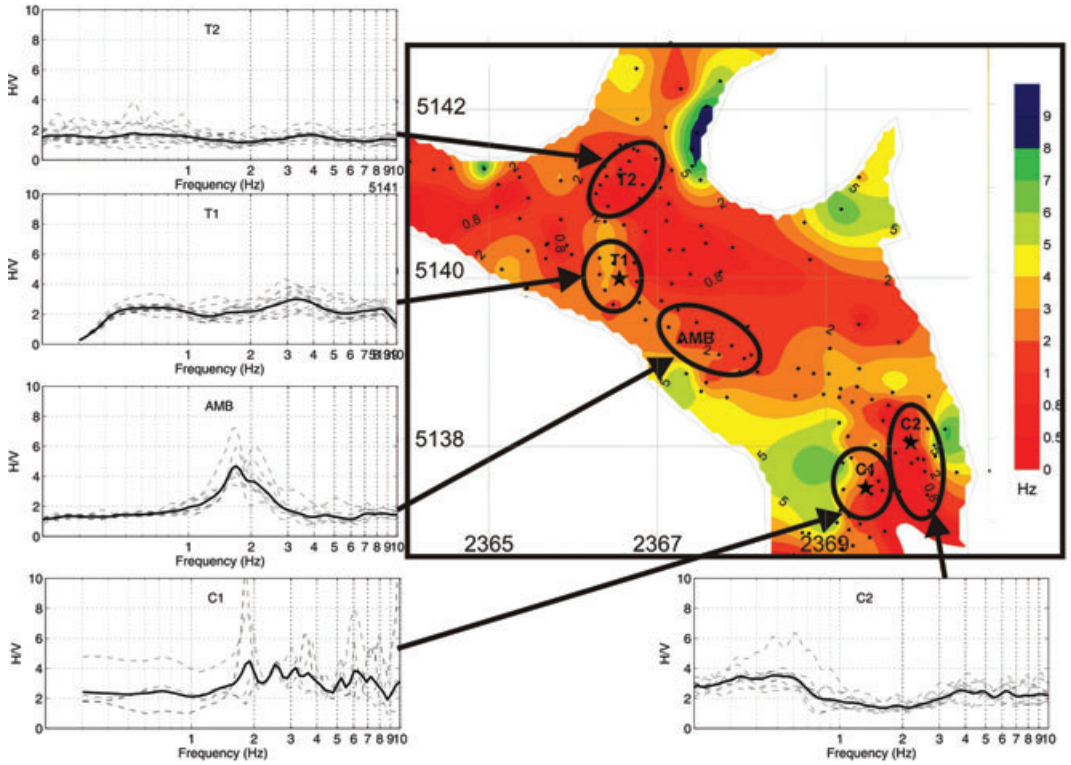

Figure 10. Right-hand panel: distribution of the fundamental frequency of vibration estimated from the HVSR of ambient noise for this study area. The panels surrounding the map show the average HVSR computed for selected zones with similar HVSR.

Fig. 10 shows the distribution of the fundamental frequency of vibration f_0 estimated from the HVSR of ambient noise as the frequency of the first HVSR peak. It must be said that, for the HVSR observed in this area, the first peak is sometimes fuzzy and it does not always correspond to the maximum HVSR amplitude. In general, the HVSR feature a single peak only in few zones, while in most cases they feature more peaks (e.g. at the valley edges) or a quite smooth behaviour. Notwithstanding, the observed HVSR feature a very good spatial coherence in the short distance range (i.e. about 200–300 m). The panels surrounding the map of Fig. 10 illustrate the situation described above. Each panel represents the average HVSR computed for selected zones with similar HVSR.

It is commonly acknowledged (e.g. Lachet & Bard 1994; Ibs-von Seht & Wohlenberg 1999; Scherbaum *et al.* 2003) that, under some assumptions about the underground structure (e.g. 1-D resonance model), the HVSR method reveals the fundamental resonance frequency of sites very easily, and the amplitude of the HVSR at the fundamental frequency f_0 is an indicator of the *S*-wave velocity contrast between bedrock and sediments (Fäh *et al.* 2001). In a complex geological setting such as that of an alpine valley, where the basic assumptions are not always satisfied, it may be trickier to distinguish between 1-D and 2-D to 3-D resonance as well as to identify the fundamental frequency of resonance. This matter will be discussed in a further section.

The fundamental frequency of resonance f_0 (Fig. 10) has been used to estimate the thickness h of the sediments within the valley. Owing to the lack of detailed data for the *S*-wave velocity, it has been preferred to use the simpler, classical formula $h_0 = Vs/(4f_0)$ valid for 1-D models, where Vs represents the average *S*-wave velocity of the sediment, to the more accurate formula based on a gradual increase of velocity with depth introduced by Ibs-von Seht & Wohlenberg (1999). Fig. 11 shows the map of the sediment thickness computed using the value of $Vs = 900\ \mathrm{m\,s^{-1}}$, estimated as the average of the *S*-wave velocity profile at site C2 located in the middle of the TRV. The estimated thickness varies from a minimum of 25 m to a maximum of about 450 m, with an error evaluated at about 20–25 per cent. The map reveals a relatively shallow sediment fill in the alluvial fan of Rivoli Bianchi and within the Tagliamento river bed (TZT in Fig. 1), while the deeper part of the valley is found at the southern part of the CCP. The results obtained here are consistent with the information of the few deep boreholes available, that are located along the But river and in Tolmezzo (Fig. 2), and where no bedrock is reached at 148 and 90 m, respectively. Note also that additional peaks in the HVSR have often been observed in similar cases and can be ascribed to surface layer with relatively high impedance contrast (e.g. Frischknecht *et al.* 2005).

6 1-D VERSUS 2-D RESPONSE FROM RESONANCE ANALYSIS

Since the 2-D resonance patterns are the results of the interference of vertical and horizontal propagating waves, they can only appear in relatively deep basins and valleys. The first attempt to parametrize the 2-D response is due to Bard & Bouchon (1985). In order to distinguish 1-D from 2-D resonance effects in a simplified way, they introduced the concept of critical shape ratio (i.e. the ratio between the maximum sediment thickness h and the valley half-width w), that, depending on the velocity contrast between sediment and bedrock, controls the kind of resonance (Fig. 12).

For valleys which have shape ratio and impedance contrast that induces 2-D resonance or other complex geometry, the approach of relating the frequency of HVSR first peak directly to 1-D frequency of resonance can lead to a wrong interpretation of the valley structure. This happens especially at valley edges or for deep and steep

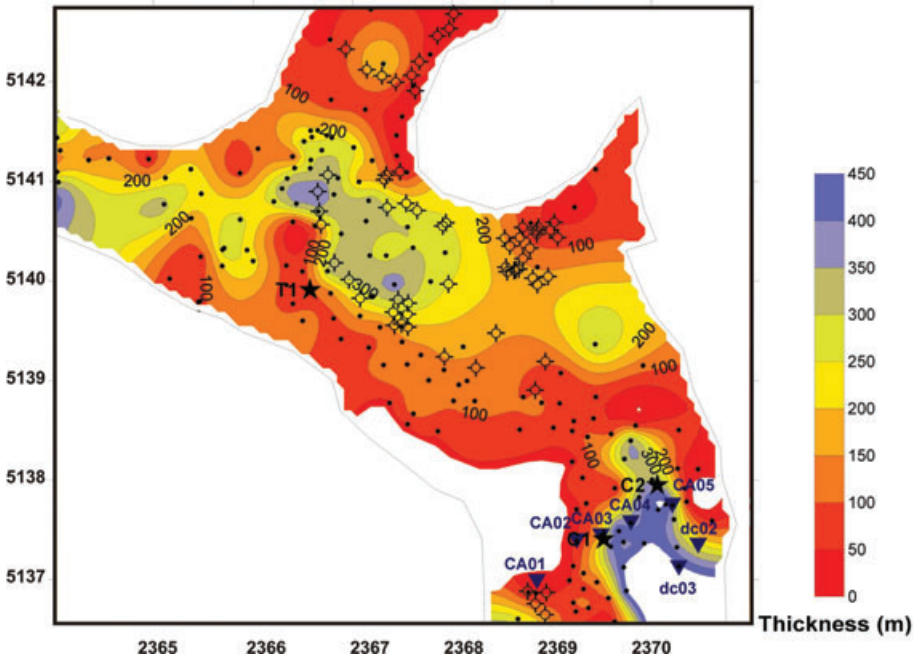

Figure 11. 3-D model of the buried morphology (i.e. thickness of the sediments above the geophysical bedrock) of the Tagliamento River Valley inferred from the interpolation both the fundamental frequency of resonance estimated from the HVSR of ambient noise and *Vs* profiles. This model can be directly compared to that displayed in Fig. 5, obtained from the gravity inversion. The white triangles indicate the array of stations used for the analysis based on the Reference Site Method. The location of the boreholes, seismic profiles and single station measurement points is also mapped.

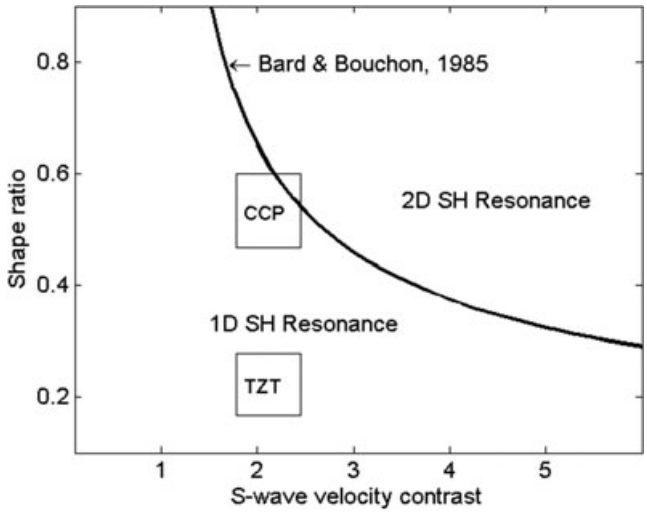

Figure 12. 1-D to 2-D critical shape ratio curve as proposed by Bard & Bouchon (1985). Rectangles represent results obtained for the cross-sections (additional panels) of the Tagliamento River Valley at TZT and CCP (see Fig. 1 for location).

basins, where the horizontally propagating surface waves interfere with vertically propagating waves (e.g. the case of the Grenoble area in Isére Valley (Gueguen *et al.* 2007) or the Rhône Valley (Frischknecht *et al.* 2005; Roten *et al.* 2006). In these cases, the 2-D resonance may become dominant and 1-D model cannot be used for interpreting the HVSR of single station measurements (Roten *et al.* 2006).

By applying Bard and Bouchon's criterion (1985) to the structure of the TRV depicted in Figs 9 or 11, it comes out (Fig. 12) that the northern part (e.g. TZT and its surroundings) features clear 1-D resonance while only in the CCP 2-D effects could arise, although neither 1-D nor 2-D resonance effects would prevail.

In order to verify the hypothesis above and evaluate the nature of the valley response in the area of CCP more accurately, two distinct methodologies have been applied, that is (1) the reference site spectral ratio method (RSSR) applied to simultaneous noise recordings as suggested by Roten *et al.* (2006) and (2) a 2-D numerical simulation of the valley response using a fast numerical method (Paolucci 1999).

6.1 The reference site spectral ratio method

The RSSR method was first developed for and applied to earthquake data (Borcherdt 1970; Lermo & Chavez-Garcia 1994). The application to noise recordings is more recent (e.g. Kagami *et al.* 1982; Kagami *et al.* 1986; Yamanaka *et al.* 1994; Steimen *et al.* 2003; Roten *et al.* 2006) and answers to the necessity of a quicker and cheaper method for estimating 2-D or 3-D amplification effects in regions with low seismicity.

The RSSR method compares the amplitude Fourier spectra of individual components recorded on a soft-soil site to those recorded at a reference station located on rock (e.g. Field *et al.* 1990; Yamanaka *et al.* 1993; Lermo & Chavez-Garcia 1994). The original method uses signals from long-distance earthquakes under the assumption that source and path effects are identical at the soil and bedrock stations. When using ambient vibrations, this important condition is not necessarily fulfilled. However, long-period microtremors are caused by oceans waves and have a long-distance source when measured in inner continental regions. Therefore, they have stable spectra for long periods of time (Bard 1998). Field & Jacob (1993) assumed that the noise spectra were white before entering the sediment valley: this condition would ensure that the source and path effects were statistically equal at the two stations over long

recording periods. According to Roten *et al.* (2006), ambient noise records recorded simultaneously by a linear array perpendicular to the valley axis can be used for identifying the resonance modes in sediment-filled valleys.

Noise records have been acquired by an array set out across the TRV in the area of CCP, where models predict the maximum thickness of the alluvial sediments (Fig. 11) and the shape ratio is supposed to be maximum. One station (CA01) was deployed nearby, on outcropping rock. CMG40 Guralp sensors with eigen frequency of 40 s have been used together with Lennartz 3-DLite/1 s sensors. About 60 min of noise wavefield were recorded. The sensors were oriented so as to have the two horizontal components aligned with the longitudinal (N150E degrees, corresponding to the valley elongation) and transversal (N60E degrees) axes of the valley, respectively. Note that the direction of the longitudinal and transversal axes of the valley correspond to the polarization direction of the Rayleigh and Love surface waves, respectively.

Fig. 13 shows the results obtained by this approach, separately for the three components, together with the HVSR computed for each single station. As already observed by other authors (e.g. Steimen *et al.* 2003), the RSSR of the horizontal components allows an easier identification of the low frequency resonance, since peaks appear sharper than those displayed by HVSR. In this case, the fundamental frequency is estimated at 0.55 and 0.6 Hz for the Love and Rayleigh waves, respectively. Note also that the fundamental peak of the horizontal components changes its characteristic frequency and amplitude across the valley, that is, as the sediment thickness changes. This fact strengthens the interpretation of a 1-D-type valley response.

6.2 Paolucci's method

In 1999, Paolucci introduced a fast method based on the Rayleigh's principle to compute the 2-D resonance frequencies of the fundamental and first higher modes, respectively, for any shape of valley and *S*-wave velocity contrast at the bedrock. This method has been applied to the transversal cross-section of the Tagliamento Valley across the CCP, which corresponds to the array described in the previous section. For major convenience, the valley profile was approximated by a cosine asymmetric shape. The valley half-width has been set at 750 m, while two different thicknesses of the sediment fill, set at 350 and 450 m have been evaluated. The corresponding shape ratio is 0.49 and 0.6, respectively. The *S*-wave velocity of the sediment fill and bedrock have been set at 900 and 1900 m s^{-1}, respectively, consistently with the average values of the three profiles available (Fig. 5). Note that, with Paolucci's method, the velocity of the bedrock does not affect the frequency of vibration but only the magnitude of the mode. We have also performed an additional test, by using a lower limit value of 600 m s^{-1} for the velocity of the sediment, in order to take into account any possible variability.

The results obtained by this analysis are summarized in Table 3. The 2-D resonance frequencies predicted for the two valley depths and the SH and SV fundamental mode of vibration (0.93, 1.07) Hz for $h = 350$ m and (0.76, 0.93) Hz for $h = 450$ m for the two modes, respectively) do not explain the values of 0.55 and 0.6 Hz estimated for the same modes from microtremors. Only using the very low limit of 600 m s^{-1} for *Vs* the 2-D resonance frequencies approach the observed ones. It comes out that the observed frequencies of resonance correspond better to a 1-D resonance of the sediment fill, rather than 2-D resonance. It also confirms what was illustrated by

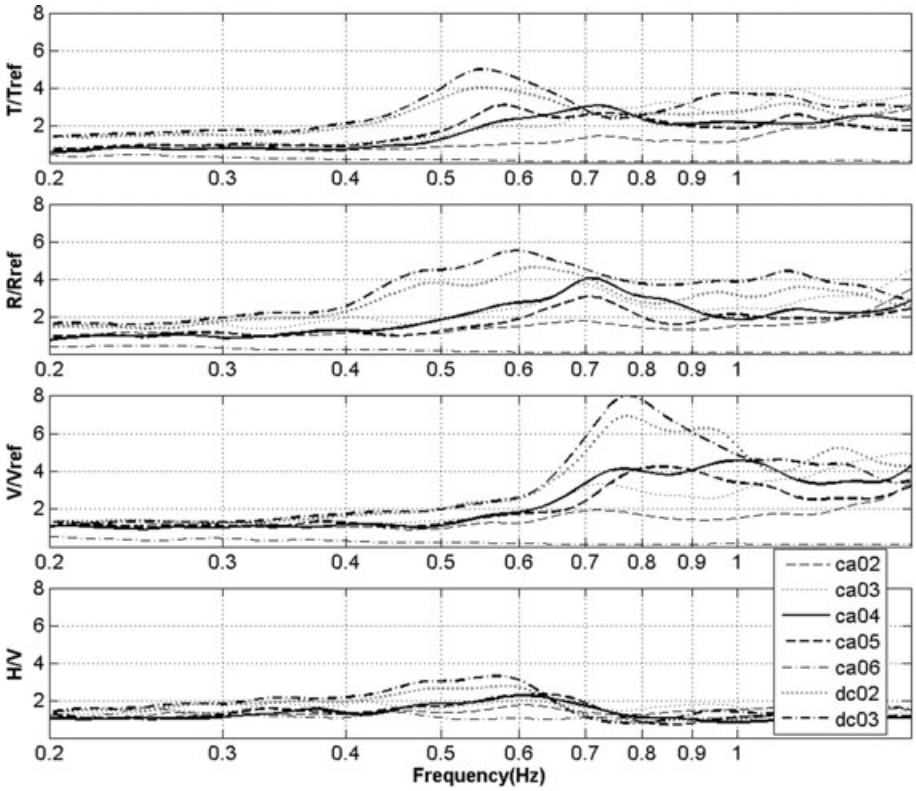

Figure 13. Spectral ratios to reference station of noise recorded along the array deployed across the Cavazzo Carnico Plain (see Figs 1 and 11). The three components of the motion are shown. The reference site is CA01. The bottom panel shows the HVSR of noise computed separately for each station of the array.

Table 3. Comparison between the resonance frequencies measured at Cavazzo Carnico Plain (CCP) and those predicted by Paolucci's method. The frequencies for the lower *Vs* velocity (i.e. 600 m s^{-1}) are indicated in brackets.

Mode	Measured	Paolucci's method $Vs = (600-)$ 900 m s^{-1}	
		$h = 350$ m	$h = 450$ m
SH	0.55 Hz	(0.61−) 0.93 Hz	(0.5−) 0.76 Hz
SV	0.6 Hz	(0.71−) 1.07 Hz	(0.62−) 0.93 Hz

Fig. 12, that is, that the seismic response of that part of CCP lies halfway between the two kinds of responses, and gives a reason for the dependency of the resonant frequency on the position of station within the valley observed in Fig. 13.

7 DISCUSSION

The main goal of this study is the definition of the buried shape of the TRV near Tolmezzo and Cavazzo Carnico municipalities (NE Italy). Due to the lack of detailed seismic reflection profiles and borehole logging data at depth, two indirect, low-cost, geophysical methods of investigation were applied, such as the gravity method and ambient noise measurements integrated by surface wave dispersion analysis. Since these two families of methods measure different physical quantities, they provide two nearly independent ways of imaging the underground morphology of the seismic bedrock. The gravity method exploits the variations in the Earth's gravitational field arising from lateral variations of the density between rocks and soils, while the seismic noise records can be used to determine the resonant frequencies of the sediments due to *S*-wave velocity contrast at the valley bottom. The surface wave dispersion analysis provides eventually a good way for constraining the *S*-wave velocity at depth locally and integrating the interpretation of the HVSR in terms of sediment thickness.

The two images of the buried topography of the TRV obtained in this study (Figs 9, 11 and 14) look reciprocally very coherent, besides some minor details. Gravity model shows a gentler shape of the valley, while that interpreted from HVSR features a stronger dependency on the data locally. It must be said, in this concern, that the construction of the latter model is based on the interpretation of the first peak frequency and that this assignation may be uncertain when the HVSR features complex shape (e.g. multiple peaks or a weak low-frequency peak). Note also, in Fig. 14, the different level of the bedrock predicted by the two methods at the western edge of profiles 4–7 that can be due to a not perfect correspondence between density and *S*-velocity of the surface structure of the model in those parts. However, being the result of independent methods, they represent the first, reliable indication on the overall underground structure of the TRV in this area. Both interpretations suffer the lack of suitable calibration points—it would be very important to have even few but well-constrained data about either the depth and the lithology of the bedrock or the density at some points, however the errors of the predicted bedrock depth have been roughly estimated in 20–25 per cent for both methods.

What is important for the gravity model is that the shape of the valley has been obtained by modelling the gravity anomalies with no heavy *a priori* assumptions. Since there is no evidence of lateral variation of the sediment density, the gravity anomaly reflects directly the average underground morphology of the density contrast at depth beneath the measurement point. The model obtained from the gravity interpretation represents a smooth image of the valley basement. It is the best result of a trial-and-error process, where the geometry of the few modelled bodies has been let vary. The differences between the measured and modelled gravity anomaly (e.g. Fig. 7e) at the edge of the valley can be interpreted as a density variation in the bedrock (i.e. the larger the measured anomaly the denser the real rock). This means that the final model here proposed (Fig. 9) could be shallower near the Curions Hill and deeper near Mt Strabut.

Some uncertainties affect the model based on the HVSR method too. The HVSR analysis of single station records can lead to an erroneous/non-unique interpretation of the fundamental resonance frequency. This may happen especially close to sharp valley edges or if the horizontal components have not previously been aligned to the valley axis. The RSSR method applied to array records has revealed a strategic tool for the overall interpretation of the resonance behaviour of the valley. In this case, it has become clear that the TRV features a prevailing 1-D response. This fact simplifies the analysis of the HVSR and allows for an easier interpretation of the resonant frequency in terms of sediment thickness.

The overall shapes of the valley obtained by the two approaches (Fig. 14) are reciprocally consistent, even though some differences exist especially where data are lacking and considering the different 'resolution power' of the methods. Both models predict the maximum sediment thickness of about 400–450 m in the area of CCP. This value seems very large if one considers that a similar thickness has been documented for the Quaternary coverage only in the southern part of the Friuli region, 50–70 km from Tolmezzo (Nicolich *et al.* 2004). It corresponds to rates of Plio-Pleistocene sedimentation which are typical of the western Alps, while they jar with the geological history of the Friuli region (Venturini, personal communication, 2007). Therefore, this depth could be consistent with that of the top of carbonate rocks. The HVSR measured of this study would confirm this hypothesis, since they show that the low frequency peak at 0.6 Hz becomes the dominant peak (Fig. 10) only in the eastern part of the valley, where the carbonate rocks are supposed to be buried under the sediments, while it is weak or lacks where conglomerates are found (e.g. North of Curions Hill).

8 CONCLUSIONS

Two passive, low-cost geophysical methods are evaluated with the aim of investigating the buried shape of the TRV in North East Italy. They are: (1) a 3-D gravimetric forward modelling and (2) the HVSR of microtremors integrated by surface wave dispersion analysis. Since these two methods measure different physical quantities, they provide two nearly independent ways of imaging the underground morphology of the seismic bedrock. The gravity data and ambient noise HVSR were interpreted separately since no joint inversion method has been developed to date for this kind of data. During this study several new data have been acquired and are presented here, that is, gravity data, seismic noise data, both at single station and array and active seismic refraction data. The latter have been used to constrain the *S*-wave velocity at depth at three sites.

The analysis and modelling of the underground structure performed by gravimetric and microtremor methods separately have lead to geophysical models (Figs 9, 11 and 14) that feature a high degree of consistency, beside some minor details. The common image thus depicted shall not be meant as a detailed and highly constrained representation of the valley bedrock; however, being the result of independent methods, it represents the first reliable reconstruction on the subsurface morphology of the TRV in the area

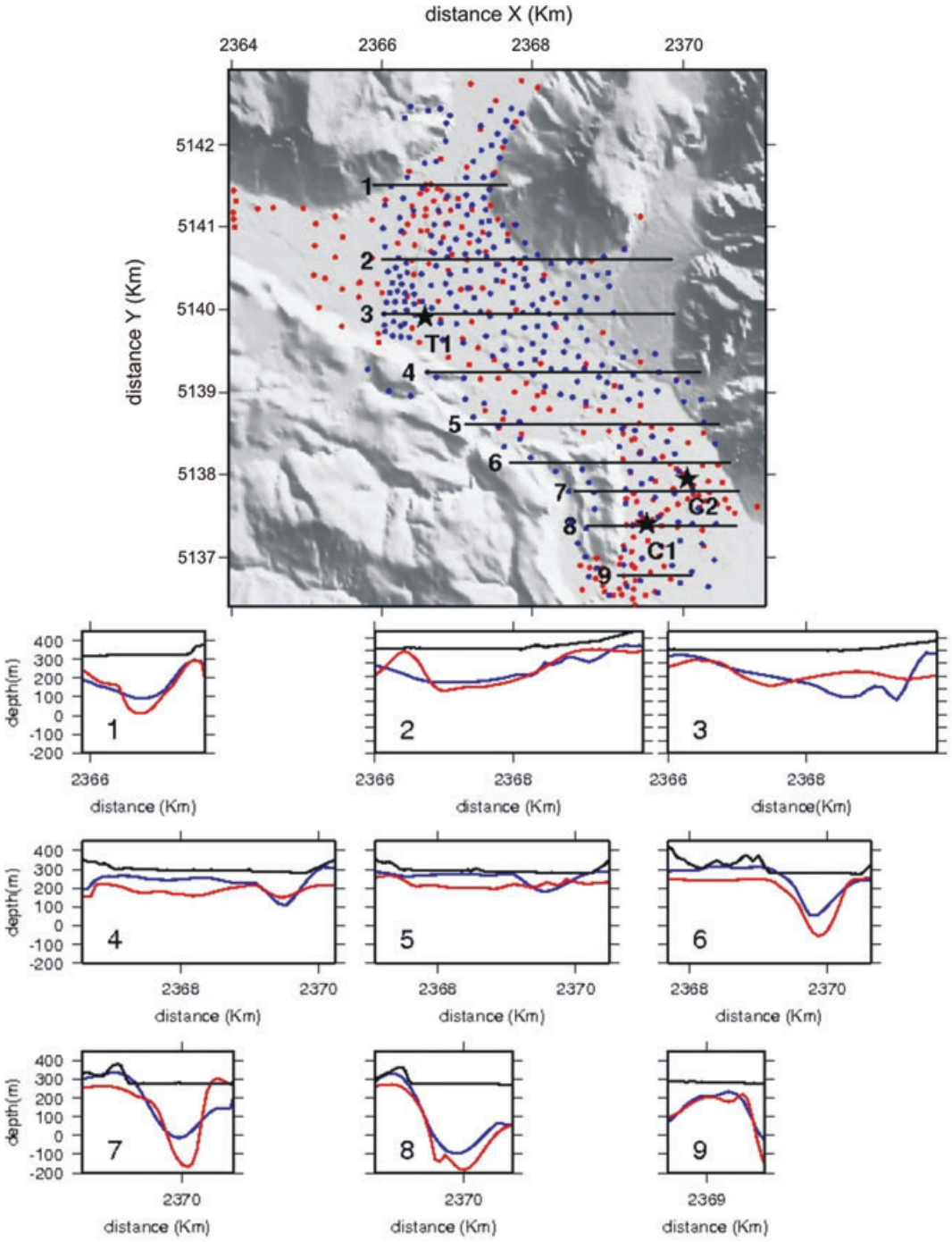

Figure 14. Comparison of the buried morphology obtained by gravity and microtremor analysis. Top panel: map of the study area with the posting of the measurement points (red for gravity and black for microtremors) and the transects along which the two models are compared. Other panels: subsurface alley bottom (elevation on the mean sea level) along the transects shown in the map (ground level in black).

surrounding the town of Tolmezzo. This image represents a useful starting point for future activities such as further surveys, numerical models, and seismic hazard or microzonation studies. Considering the very low-impact of these methods, the overall approach of a joint application of gravimetric and microtremor surveys is confirmed as a powerful tool of investigation for the aims above depicted.

The basin of the TRV in this area features a width ranging from about 750 m to 2.5 km. The bedrock morphology features two main trenches (Fig. 11). That located in the area of Tolmezzo is wider and has an average depth of about 200–300 m; the other, located beneath the CCP, is much narrower and deeper and it reaches a depth of about 400–450 m. This value seems very large for the eastern Alps and could correspond to the top of carbonate rocks. The two trenches are separated by a saddle that joins the Curions Hill to the foot of Mt Amariana where the sediment thickness decreases to less than 100 m.

On the basis of the obtained morphology and some direct measurements, it comes out that the TRV features an overall 1-D seismic response (i.e. the resonance is related only to the sediment thickness and not to the cross-section shape). Even in its deepest

part, that is, the area of the CCP, the 1-D resonance is well documented although some limited 2-D effects could probably take place here in addition.

ACKNOWLEDGMENTS

We are grateful to C. Venturini and M. Ponton for the useful discussion about the geology of the study area. We would like to thank also G. Bressan for several fruitful discussions. We are grateful to Hans Pfister for having informed us on the preliminary results obtained by his GPR survey in CCP. We also thank Roberto Paolucci for having supplied us with the code of his numerical method based on the Rayleigh principle. Normal-mode and phase-velocity stack computations were performed by using Computer Programs in Seismology, version 3.30 (2005) developed by Robert Herrmann. Several figures were drawn by using GMT software (Wessel & Smith 1998). The paper has been improved also thanks to the constructive comments of two anonymous reviewers. We acknowledge their effort.

This research was partly funded by the European Union under the INTERREG IIIB-Alpine Space framework, project no. F/I-2/3.325 entitled 'SISMOVALP – Seismic hazard and alpine valley response analysis', and the Italian Ministry of the University and Research (MIUR) under the PRIN 2007 framework, project no. 2007PTRC4C_005 entitled 'Comparison between direct and indirect, low-impact methods for accurate estimation and parametrization of the seismic site response'.

REFERENCE

Akamatsu, J., Fujita, M. & Nishimura, K., 1992. Vibration characteristics of microseisms and their applicability to microzoning, *J. Phys. Earth,* **40,** 137–150.

Aki, K., 1993. Local site effects on weak and strong ground motion, *Tectonophysics,* **218,** 93–111.

Ambraseys, N.N., 1976. The Gemona di Friuli earthquake of 6 May 1976, in *The Gemona di Friuli Earthquake of 6 May 1976, Part 2,* eds Picard, P., Ambraseys, N.N. & Ziogas, G.N., UNESCO, Restricted Technical Report RP/1975–76 2.222.3., Paris.

Banerjee, B. & Das Gupta, S.P., 1977. Short note on gravitational attraction of rectangular parallelepiped, *Geophysics,* **42**(5), 1053–1055.

Bard, P.Y. & Bouchon, M., 1985. The two-dimensional resonance of sediment-filled valleys, part II: The case of incident P and SV waves, *Bull. seism. Soc. Am.,* **75,** 519–541.

Bard, P.-Y., 1998. Microtremor measurement: a tool for site effect estimation? in *Proceedings of the Effects of Surface Geology on Seismic Motion,* pp. 1251–1279, eds Irikura, K., Kudo, K., Okada, H. & Sasatani, T., Balkema, Rotterdam.

Bard, P.-Y. & SESAME Participants, 2004. The SESAME project: an overview and main results, in *Proceedings of the 13th World Conf. Earth. Engng.,* Vancouver, August 2004, Paper # 2207.

Bindi, D., Parolai, S., Enotarpi, M., Spallarossa, D., Augliera, P. & Cattaneo, M., 2001. Microtremor H/V spectral ratio in two sediment-filled valleys in western Liguria (Italy), *Boll. Geof. Teor. Appl.,* **42**(3–4), 305–315.

Bonilla, L.F., Steidl, J.H., Lindley, G.T, Tumarkin, A.G. & Archuleta, R.J, 1997. Site amplification in the San Fernando valley, California: variability of site-effect estimation using the S-wave, coda, and H/V methods, *Bull. seism. Soc. Am.,* **87,** 710–730.

Bonnefoy-Claudet, S., Cotton, F. & Bard, P.-Y., 2006. The nature of noise wavefield and its applications for site effects studies. A literature review, *Earth-Sci. Rev.,* **79**(3–4), 205–227.

Borcherdt, R.D., Glassmoyer, G., Der Kiureghian, A. & Cranswick, E., 1989. Results and data from seismologic and geologic studies following earthquakes of December 7, 1988 near Spitak, Armenia, S.S.R., U.S. Geol. Surv. Open-File Rept. 89–163A.

Borcherdt, R.D., 1970. Effects of local geology on ground motion near San Francisco Bay, *Bull. seism. Soc. Am.,* **60,** 29–61.

Braitenberg, C., Ebbing, J. & Götze, H.-J., 2002. Inverse modelling of elastic thickness by convolution method–the Eastern Alps as a case example, *Earth planet. Sci. Lett.,* **202,** 387–404.

Bressan, G., 1981. Morphological elements and seismotectonic behaviour in Cavazzo Carnico and Trasaghis area, *Master thesis,* University of Trieste, unpublished (in Italian).

Brocher, T.M., 2005. Empirical relations between elastic wave speeds and density in the Earth's crust, *Bull. seism. Soc. Am.,* **95,** 2081–2092.

Carniel, R., Barazza, F. & Pascolo, P., 2006. Improvement of Nakamura technique by singular spectrum analysis, *Soil Dyn. Earthq. Eng.,* **26,** 55–63.

Carniel, R., Malisan, P., Barazza, F. & Grimaz, S., 2008. Improvement of Nakamura technique by wavelet analysis, *Soil Dyn. Earthq. Eng.,* **28,** 321–327.

Carulli, G.B. & Ponton, M., 2002. Le alpi Carniche meridionali (o Alpi Tolmezzine), in *Alpi e Prealpi Carniche e Giulie. Soc. Geol. It.,* BE-MA Editrice.

Carulli, G.B., 2000. Il nodo tettonico di Tolmezzo e la struttura del Mt. Amariana, in *Guida alla Escursioni, 80a Riunione Estiva S.G.I.,* 6–8 September, Trieste, Italy, pp. 70–73.

Carulli, G.B., 2007. *Geological map of the Friuli Venezia Giuli region,* SELCa, Firenze, Italy.

Cercato, M., 2009. Addressing non-uniqueness in linearized multichannel surface wave inversion, *Geophys. Prospect.,* **57,** 27–47.

Delgado, J., Lopez Casado, C., Ginger, J., Cuenca, A. & Molina, S., 2000. Microtremors as a geophysical exploration tool: applications and limitations, *Pure appl. Geophys.,* **157,** 1445–1462.

Di Giacomo, D., Gallipoli, M.R., Mucciarelli, M., Parolai, S. & Richwalski, S.M., 2005. Analysis and modeling of HVSR in the presence of a velocity inversion: the case of Venosa, Italy, *Bull. seism. Soc. Am.,* **95**(6), 2364–2372.

Ebbing, J., Braitenberg, C. & Götze, H.-J., 2005. The lithospheric density structure of the Eastern Alps, *Tectonophysics,* **414,** 145–155.

Faccenda, M., Bressan, G. & Burlini, L., 2007. Seismic properties of the upper crust in the central Friuli area (north eastern Italy) based on petrophysical data, *Tectonophysics,* **445,** 210–226.

Faccioli, E., 1991. Seismic amplification in the presence of geological and topographic irregularities, In *Proceedings of the 2nd International conference on Recent Advances in Geotechnical Earthquake Engineering and Soil Dynamics,* St Louis, pp. 1779–1797.

Fäh, D., Kind, F. & Giardini, D., 2001. A theoretical investigation of average H/V ratios, *Geophys. J. Int.,* **145,** 535–549.

Fäh, D., Kind, F. & Giardini, D., 2003. Inversion of local S-wave velocity structures from average H/V ratios, and their use for the estimation of site-effects, *J. Seismol.,* **7,** 449–467.

Fäh, D., Theodulidis, N. & Savvaidis, A., 2007. Inversion of local S-wave velocity structure from average H/V ratios and comparison with cross-hole measurements, in *Proceedings of the 4th International Conference on Earthquake Geotechnical Engineering,* June 25–28, 2007, Thessalonica, Greece. Paper No. 1410.

Field, E.H., 1996. Spectral amplification in a sedimentary-filled valley exhibiting clear basin-edgeinduced waves, *Bull. seism. Soc. Am.,* **86,** 991–1005.

Field, E.H. & Jacob, K.H., 1993. The theoretical response of sedimentary layers to ambient seismic noise, *Geophys. Res. Lett.,* **20,** 2925–2928.

Field, E.H., Hough, S.E. & Jacob, K.H., 1990. Using microtremors to assess potential earthquake site response: a case study in flushing meadows, New York City, *Bull. seism. Soc. Am.,* **80,** 1456–1480.

Frischknecht, C., Rosset, P. & Wagner, L.L., 2005. Toward seismic microzonation -2D modelling and ambient seismic noise measurements: the case of an embanked, deep alpine valley, *Earthq. Spectra,* **21**(3), 156–536.

Frischknecht, C. & Wagner, L.L., 2004. Seismic soil effect in an embanked deep alpine valley: a numerical investigation of two-dimensional resonance, *Bull. seism. Soc. Am.,* **94/1,** 681–171.

Gardner, G.H.F., Gardner, L.W. & Gregory, A.R., 1974. Formation velocity and density–The diagnostic basic for stratigraphic traps, *Geophysics,* **39,** 770–780.

Gotze, H.J. & Schmidt, S., 2005. IGMAS URL: www.gravity.uni-kiel.de/igmas.

Gotze, H.J., 1978. Ein numerisches verfahren zur berechung der gravimetrischen feldgrossen dreidimensionaler modellkorper, *Arch. Met. Geoph. Biokl., Ser. A,* **25,** 195–215.

Gueguen, P., Cornou, C., Garambois, S. & Baton, J., 2007. On limitation of the H/V spectral ratio using seismic noise as an exploration tool: application to the Grenoble valley (France), a small apex ratio basin, *Pure appl. Geophys.,* **164,** 115–134.

Havenith, H.B, Faeh, D., Polom, U. & Roulè, A., 2007. S-wave velocity measurements applied to the microzonation of Basel, Upper Rhine Graben, *Geophys. J. Int.,* **170,** 346–358.

Herak, M., 2008. ModelHVSR–A Matlab tool to model horizontal-to-vertical spectral ratio of ambient noise, *Comput. Geosci.,* **34,** 1514–1526.

Herrmann, R.B., 2005. Computer Programs in Seismology, Version 3.30, Saint Louis University.

Herrmann, R.B. & Ammon, C.J., 2002. Surface waves, receiver functions and crustal structure, Computer Programs in Seismology Version 3.30.

Hayashi, K., Matsuoka, T. & Hatakeyama, H., 2005. Joint Analysis of a Surface-wave Method and Micro-gravity Survey, *J. Environ. Eng. Geophys.,* **10,** 175–184, doi:10.2113/JEEG10.2.175.

Ibs-von Seht, M. & Wohlenberg, J., 1999. Microtremor measurements used to map thickness of soft sediments, *Bull. seism. Soc. Am.,* **89,** 250–259.

Kagami, H., Okada, S., Shiono, K., Oner, M., Dravinski, M. & Mal, A.K., 1986. Observation of 1 to 5 second microtremors and their application to earthquake engineering. Part III. A two-dimensional study of site effects in S. Femando valley, *Bull. seism. Soc. Am.,* **76,** 1801–1812.

Kagami, H., Duke, C.M., Liang, G.C. & Ohta, Y., 1982. Observations of 1-to 5 seconds microtremors and their application to earthquake engineering. Part II: Evaluation of site effect upon seismic wave amplification due to extremetly deep soil deposits, *Bull. seism. Soc. Am.,* **72,** 987–998.

Kanai, K. & Tanaka, T., 1961. On microtremors, *VIII. Bull. Earthq. Res. Inst.,* **39,** 97–114.

Lacave, C. *et al*., 2006. Generic Alpine Valley characterization, CD-ROM II, Projet Interreg 3B, Sismovalp.

Lacave, C. & Lemeille, F., 2007. Seismic hazard and alpine valley response analysis: generic valley configurations, in *First European Conference on Earthquake Engineering and Seismology,* pp. 1–6, Geneva, Switzerland, 3–8 September 2006.

Lachet, C. & Bard, P.Y., 1994. Numerical and theoretical investigations on the possibilities and limitation of Nakamura's technique, *J. Phys. Earth,* **42,** 377–397.

La Fehr, T.R., 1991a. Standardization in gravity redaction, *Geophysics,* **56**(8), 1170–1178.

La Fehr, T.R., 1991b. An extract solution for the gravity curvature (Bullard B), *Geophysics,* **56**(8), 1179–1184.

Lemeille, F., 2004. Contribution de l'IRSN à la synthèse des éléments généraux sur la géométrie et sur la nature du remplissage des vallées alpines–Projet Européen Sismovalp/Interreg III WP04 (NT n°04–50), Fontenay-aux-Roses, IRSN, 22 pp.

Lermo, J. & Chavez-Garcia, F.J., 1994. Are microtremors useful in site response evaluation? *Bull. seism. Soc. Am.,* **84**(5), 1350–1364.

Lermo, J. & Chavez-Garcia, F.J., 1993. Site effect evaluation using spectral ratios with only one station, *Bull. seism. Soc. Am.,* **83,** 1574–1594.

Luke, B., Calderon-Macias, C., 2007. Inversion of seismic surface wave data to resolve complex profiles, *J. Geotech. Geoenviron. Eng.,* **133,** 155–165.

Maceira, M. & Ammon, C.J., 2009. Joint inversion of surface wave velocity and gravity observations and its application to central Asian basins shear velocity structure, *J. geophys. Res.,* **114,** B02314, doi:10.1029/2007JB005157.

McMechan, G.A. & Yedlin, M.J., 1981. Analysis of dispersive waves by wave field transformation, *Geophysics,* **46,** 869–874.

Møller, M.J., Olsen, H., Ploug, C., Strykowski, G. & Hjorth, H., 2007. Gravity field separation and mapping of buried quaternary valleys in Lolland, Denmark using old geophysical data, *J. Geodyn.,* **43,** 330–337.

Nakamura, Y., 1989. A method for dynamic characteristic estimations of subsurface using microtremors on ground surface, *Q. Rept. RTRI Jpn.,* **30,** 25–33.

Nicolich, R., Della Vedova, B., Giustiniani, M. & Fantoni, R., 2004. Carta del suolo della pianura friulana. Reg. Auton. Friuli Venezia Giulia, Direz. Centr, Ambiente e Lavori Pubblici, Servizio Geologico, L.A.C., Firenze.

Nishida, R., Munetou, H., Nakamura, H., Ueda, T., Nishiyama, H. & Noguchi, T., 2001. Subsurface structure analysis by gravity survey, *Reports of the 53rd Japan Society of Civil Engineering Chugoku Branch Conference,* I-48, 95 (in Japanese).

Noganoh, M., Kagami, H. & Muratami, H., 1993. Effects of surface and subsurface irregularities, in *Earthquake Motions and Ground Conditions,* Chapter 3.3, Tokyo, Architectural Institute of Japan.

Noguchi, T. & Nishida, R., 2002. Determination of subsurface of Tottori Plain using microtremors and gravity anomaly, *J. Nat. Dis. Sc.,* **24,** 1–13.

Ohta, Y., Kagami, H., Goto, N. & Kudo, K., 1978. Observations of 1-to 5-second microtremors and their application to earthquake engineering. Part I: Comparison with long-period accelerations at the Tokachi-Oki earthquake of 1968, *Bull. seism. Soc. Am.,* **68,** 767–779.

Paolucci, R., 1999. Shear resonance frequencies of alluvial valleys by Rayleigh's method, *Earthq. Spectra,* **15**(3), 503–521.

Parolai, S., Bormann, P. & Milkereit, C., 2002. New relationships between *Vs*, thickness of sediments, and resonance frequency calculated by the H/V ratio of seismic noise for the Cologne area (Germany), *BSSA,* **92,** 2521–2527.

Parolai, S., Richwalski, S.M., Milkereit, C. & Bormann, P., 2004. Assessment of the stability of H/V spectral ratios from ambient noise and comparison with earthquake data in the Cologne area (Germany), *Tectonophysics,* **390,** 57–73.

Pedersen, H.A., Campillo, M. & Sanchez-Sesma, F.J., 1995, Azimuth dependent wave amplification in alluvial valleys, *Soil Dyn. Earthq. Eng.,* **14,** 289–300.

Petris, P., 1996. Studio geologico, in *Piano regolatore generale comunale,* Tolmezzo, Udine, Italy.

Priolo, E., Michelini, A., Laurenzano, G., Addìa, R. & Puglia, A., 2001. Seismic response from microtremors in Catania (Sicily, Italy), *Boll. Geof. Teor. Appl.,* **42,** 335–359.

Roten, D., Fäh, D., Cornou, C. & Giardini, D., 2006. 2D resonances in Alpine valleys identified from ambient vibration wavefields, *Geophys. J. Int.,* **165,** 889–905.

Sanchez-Sesma, F.J., Ramos-Martinez, J. & Campillo, M., 1993. An indirect boundary element method applied to simulate the seismic response of alluvial valleys for incidence of P, S and Rayleigh waves, *Earthq. Eng. Struct. Dyn.,* **22,** 279–295.

Scherbaum, F., Hinzien, K.G. & Ohrnberger, M., 2003. Determination of shallow shear-wave velocity profiles in the Cologne/Germany area using ambient vibrations, *Geophys. J. Int.,* **152,** 597–612.

SESAME Project, 2004. Guidelines for the implementation of the H/V spectral ratio technique on ambient vibrations measurements, processing and interpretation, SESAME European research project; WP12–Deliverable D23.12. European Commission–Research General Directorate. Project No. EVG1-CT-2000–00026 SESAME. December 2004.

SISMOVALP Project–WP6 Generic alpine ground motion, 2007. A 2D Simulation benchmark for the study of the seismic response of alpine valley, Notebook report prepared by E. Priolo and G. Laurenzano with the contribution of all WP6 participants. Unpublished document.

Sing, S.K., Lermo, J., Dominguez, T., Ordaz, M., Espinosa, J.M., Mena, E. & Quass, R., 1988. The Mexico earthquake of September 19, 1985-a study of amplification of seismic waves in the valley of Mexico with respect to a hill zone site, *Earthq. Spectra,* **4,** 653–673.

Slejko, D. *et al*., 1987. Modello sismotettonico dell'Italia Nord-Orientale, C.N.R. G.N.D.T. Rendiconto n. 1, Trieste, 83 pp.

Steimen, S., Fäh, D., Kind, F., Schmid, C. & Giardini, D., 2003. Identifying 2D resonance in microtremor wave fields, *Bull. seism. Soc. Am.,* **93,** 583–599.

Tokimatsu, K., Arai, H. & Asaka, Y., 1997. Deep shear-wave structure and earthquake ground motion characteristics in Sumiyoshi area, Kobe

city, based on microtremor measurements., *J. Struct. Constr. Architectural Institute Japan,* **491,** 37–45 (in Japanese).

Uebayashi, H., 2003. Extrapolation of irregular subsurface structures using the horizontal to vertical spectral ratio of long period microtremors, *Bull. seism. Soc. Am.,* **93**(2), 570–582.

Vallon, M., 1999. Estimation de l'épaisseur d'alluvions et sédiments quaternaires dans la region grenobloise par inversion des anomalies gravimétriques, IRSN/CNRS Internal Report, 34 pp. (in French).

Yamanaka, H., Takemura, M., Ishida, H. & Niwa, M., 1994. Characteristics of long-period microtremors and their applicability in exploration of deep sedimentary layers, *Bull. seism. Soc. Am.,* **84,** 1831–1831.

Yamanaka, H., Dravinski, M. & Kagami, H., 1993. Continous measurements of microtremors on sediments and basament in Los Angeles, California, *Bull. seism. Soc. Am.,* **83,** 1595–1609.

Wessel, P. & Smith, H.F., 1998. New, improved version of Generic Mapping Tools released, *EOS Trans. AGU,* **79,** 579.

Xia, J., Miller, R.D. & Park, C.B., 1999. Estimation of near-surface shear wave velocity by inversion of Rayleigh waves, *Geophysics,* **64,** 691–700.

Zanolla, C. *et al*., 2005. New gravity maps of the Eastern Alps and significance for the crustal structures, *Tectonophysics,* **414,** 127–143.